HHS Public Access

Author manuscript

Mol Microbiol. Author manuscript; available in PMC 2019 October 03.

Published in final edited form as:

Mol Microbiol. 2018 October ; 110(2): 239–261. doi:10.1111/mmi.14100.

Rhodobacterales use a unique L-threonine kinase for the assembly of the nucleotide loop of coenzyme B_{12}

Norbert K. Tavares, **Chelsey M. VanDrisse**, and **Prof. Jorge C. Escalante-Semerena***

Department of Microbiology, University of Georgia

Abstract

Several of the enzymes involved in the conversion of adenosylcobyric acid (AdoCby) to adenosylcobamide (AdoCba) are yet to be identified and characterized in some cobamide (Cba)-producing prokaryotes. Using a bioinformatics approach, we identified the *bluE* gene (locus tag RSP_0788) of *Rhodobacter sphaeroides* 2.4.1 as a putative functional homologue of the L-threonine kinase enzyme (PduX, EC 2.7.1.177) of *S. enterica*. In AdoCba, (*R*)-1-aminopropan-2-ol *O*-phosphate (AP-P) links the nucleotide loop to the corrin ring; most known AdoCba producers derive AP-P from L-Thr-*O*-3-phosphate (L-Thr-P). Here, we show that *Rs*BluE has L-Thr independent ATPase activity *in vivo* and *in vitro*. We used ^{31}P-NMR spectroscopy to show that *Rs*BluE generates L-Thr-P at the expense of ATP and is unable to use L-Ser as substrate. BluE from *R. sphaeroides* or *Rhodobacter capsulatus* restored AdoCba biosynthesis in *S. enterica* Δ*pduX* and *R. sphaeroides* Δ*bluE* mutant strains. *R. sphaeroides* Δ*bluE* strains exhibited a decreased pigment phenotype that was restored by complementation with BluE. Finally, phylogenetic analyses revealed that *bluE* was restricted to the genomes of a few *Rhodobacterales* that appear to have a preference for a specific form of Cba, namely *Coα*-(α−5,6-dimethylbenzimidazolyl-*Coβ*-adenosylcobamide (a.k.a. adenosylcobalamin, AdoCbl; coenzyme B_{12}, CoB_{12}).

Abbreviated summary

Aminopropanol-phosphate (AP-P) links the nucleotide loop to the ring in vitamin B_{12}. The PduX enzyme is the kinase that is commonly responsible converting L-Thr to L-Thr-P, which is in turn decarboxylated to make AP-P. *Rhodobacterales* lack *pduX*. Instead they have the non-orthologous *bluE* gene that encodes an enzyme that, unlike PduX, is specific for L-Thr and cannot use L-Ser. Phylogenetic analysis show that *bluE* is restricted to the *Rhodobacterales*.

BluE, a new class of L-Thr kinases found in *Rhodobacterales*

*Corresponding author: Department of Microbiology, University of Georgia, 212C Biological Sciences Building, 120 Cedar Street, Athens, GA 30602. Phone: +1 (706) 542-2651, Fax: +1 (706) 542-2815 jcescala@uga.edu.

Introduction

Bacteria and archaea that synthesize cobamides (Cbas) use one of two pathways, the O_2-dependent or O_2-independent pathway (Blanche *et al.*, 1993, Roessner *et al.*, 2001) [reviewed in (Escalante-Semerena & Warren, 2008)]. There are several differences between these pathways, but the one that is most frequently used to distinguish one from the other is the timing of insertion of the cobalt ion into the tetrapyrrole ring. In the O_2-dependent pathway, cobalt insertion occurs late in the branch of the pathway that assembles the corrin ring. In contrast, in the O_2-independent pathway cobalt insertion occurs at the second committed step of the corrin ring biosynthetic pathway (Fig. 1). For this reason, the pathways are also referred to as the late- and early-cobalt insertion pathways. The early-Co-insertion pathway has been extensively studied in *Salmonella enterica* sv. Typhimurium LT2 [reviewed in (Escalante-Semerena, 2007, Escalante-Semerena & Warren, 2008)] and *Bacillus megaterium* (Biedendieck *et al.*, 2010, Collins *et al.*, 2013, Beck *et al.*, 1997, Leech *et al.*, 2002, Raux *et al.*, 1998). In this pathway, *de novo* synthesis of the corrin ring occurs only in the absence of oxygen due to the oxygen lability of precorrin 5B (Moore *et al.*, 2013), the product of the cobalt-precorrin 5A acylhydrolase (CbiG) enzyme (Schroeder *et al.*, 2009). The late-Co-insertion pathway is functional under normoxic and anoxic conditions, and has been primarily studied in *Pseudomonas denitrificans* (Blanche *et al.*, 1991, Cameron *et al.*, 1991b, Cameron *et al.*, 1991a, Crouzet *et al.*, 1990, Debussche *et al.*, 1991, Thibaut *et al.*, 1990, Zumft, 1997) and *Rhodobacter capsulatus* (Biel, 1992, Heldt *et al.*, 2005, McGoldrick *et al.*, 2005, Pollich & Klug, 1995, Vlcek *et al.*, 1997). Both pathways share several homologous enzymes, however, while most of the enzymes within the early-Co-insertion pathway of *S. enterica* have been identified, the functional equivalents of some enzymes have not been identified in the late-Co-insertion pathway. For example, it is not known which phosphatase dephosphorylates adenosylcobalamin-phosphate (AdoCbl-P) to produce the final product, adenosylcobalamin (AdoCbl). Also unknown is the kinase that generates L-Thr-P, which is converted to (*R*)-1-aminopropan-2-ol *O*-phosphate (a.k.a (*R*)-1-amino-2-propanol-*O*-2-phosphate, AP-P), which tethers the nucleotide loop to the corrin ring (Fig. 1, highlighted red). In *S. enterica*, PduX (locus tag STM2058, hereafter *Se*PduX) phosphorylates L-Thr (Fan & Bobik, 2008, Fan *et al.*, 2009). Notably, the functional equivalent of *Se*PduX has not been identified in any organism that uses the late-Co-insertion pathway.

The *bluE* gene was identified in *R. capsulatus*, BB1 as the second gene in an operon named *bluFEDCB* (Fig. 1) because disruption of the operon resulted in a reduction of red pigmentation or a “blush” phenotype (Pollich & Klug, 1995). In *R. capsulatus* precursor molecules of the initial steps for AdoCbl synthesis enters the bacteriochlorophyll (Bch) synthesis pathway and are incorporated into bacteriochlorophyll (Willows & Kriegel, 2009). In addition, AdoCbl is a required cofactor for enzymes that synthesize bacteriochlorophyll such as BchE/ChlE and is needed for transcriptional activation of genes that lead to carotenoid biosynthesis (Yin & Bauer, 2013, Gough *et al.*, 2000). Therefore, cells with incomplete AdoCbl production have a pigmentation phenotype (Yin & Bauer, 2013). Disruption of the *bluE* gene by a Tn*5* element blocked AdoCbl biosynthesis resulting in an auxotrophy and blush phenotype that was corrected by cobalamin (Cbl) but not by

cobinamide (Cbi), a Cbl precursor (Fig. 1) (Pollich & Klug, 1995). BluD is homologous to the AdoCbi-P synthase (CbiB, EC 6.3.1.10) of *S. enterica*, (CobD in the late-Co-insertion pathway), BluC is homologous to the L-Thr-P decarboxylase (CobD, EC 4.1.1.81) of *S. enterica*, (CobC in the late-Co-insertion pathway), and BluB was later identified in *Sinorhizobium meliloti* and *Rhodospirillum rubrum* as a 5,6-dimethylbenzimidazole (DMB) synthase (Gray & Escalante-Semerena, 2007, Campbell *et al.*, 2006, Taga *et al.*, 2007). BluB activity has not been identified in *S. enterica*. To date, the putative functions of the proteins encoded by the *bluF* and *bluE* genes have not been identified. BluF is likely the last missing enzyme in the late-Co-insertion pathway (Pollich *et al.*, 1996), the AdoCbl-P phosphatase (CobC) of *S. enterica* (Zayas & Escalante-Semerena, 2007) (unpublished data). Here we report the identification and initial characterization of BluE (locus tag RSP_0788). Our data support the conclusion that BluE is the L-threonine (L-Thr) kinase of *Rhodobacter sphaeroides* 2.4.1.

We found that *Rs*BluE failed to use L-Ser as substrate to produce L-Ser-P. L-Ser-P is used by some Cba producing organisms such as *Sulfurospirillum multivorans* to make ethanolamine phosphate (EA-P) (Keller *et al.*, 2016), which serves as the nucleotide loop linker in norCbas (*e.g.* *Co*α−5,6-dimethylbenzimidazolyl-176-cobamide, norCbl, norB$_{12}$). (Kräutler *et al.*, 2003). NorCbas have a nucleotide loop linker that lacks a methyl group at position 176. The *S. multivorans* L-Ser-P/L-Thr-P decarboxylase, CobD (locus tag SMUL_1544) preferentially uses L-Ser-P over L-Thr-P (Keller *et al.*, 2016) to produce EA-P. *S. multivorans* naturally produces norpseudo-Cbl (Coα-adeninyl-176-norcobamide, norpseudo-B$_{12}$) because the Cba-dependent PCE reductive dehalogenase (PceA) enzymes in *S. multivorans* has a preference for norCbas (Keller *et al.*, 2018, Keller *et al.*, 2013) and norpseudo-Cbas in particular (Keller *et al.*, 2018, Keller *et al.*, 2014, Keller *et al.*, 2013, Kräutler *et al.*, 2003). Pseudo-Cbas are cobamides with adenine as the lower axial ligand, as opposed to DMB in Cbl. The enzyme that generates L-Ser-P has not been identified in *S. enterica* or *S. multivorans* and it appears *R. sphaeroides* cannot incorporate L-Ser-P into Cba synthesis via BluE.

Lastly, the *Rs*BluE enzyme was found to be restricted to a subclass of *Rhodobacterales* with genetic attributes that indicate they have a strong preference for AdoCbl. That is to say, these *Rhodobacter* species prefer and synthesize only a Cba with DMB as the lower ligand base and AP-P as the nucleotide linker; *Co*α-(α−5,6-dimethylbenzimidazolyl-*Co*β-adenosylcobamide (a.k.a. adenosylcobalamin, AdoCbl; coenzyme B$_{12}$, CoB$_{12}$).

Results

BluE is the L-Thr kinase involved in AdoCbl biosynthesis in *Rhodobacterales*.

Previous bioinformatics analysis of the genomes of AdoCba producers (Rodionov *et al.*, 2003) did not identify homologues of the L-Thr kinase (PduX in *S. enterica*, *Se*PduX) in organisms that use the late-cobalt-insertion pathway for AdoCbl biosynthesis (Fig. 1A). Because of significant protein sequence differences, BLASTP (Altschul *et al.*, 1997) searches using *Se*PduX failed to retrieve BluE sequences and *vice versa*. The *bluE* (locus RCAP_rcc02055, accession number Z46611) gene from *R. capsulatus* was first identified as part of an AdoCbl biosynthetic gene cluster but its function was not elucidated (Pollich &

Klug, 1995). All *bluE* homologues identified thus far have been found clustered with other AdoCbl biosynthetic genes. BluE proteins were on average about 23–35 residues (5–6 kDa) shorter than *Se*PduX (Fig. 2). The BluE proteins from *R. capsulatus* SB1003 (*Rc*BluE; 27 kDa, 265 amino acids) and *R. sphaeroides* (*Rs*BluE, locus RSP_0788; 28 kDa, 277 amino acids) displayed 47–52% end-to-end identity among the *Rhodobacterales* analyzed (Fig. 2), but only a 19% identity to *Se*PduX (33 kDa, 300 amino acids). This generally falls below the threshold of most default BLAST queries, and it is likely the reason why it was overlooked in previous bioinformatics analysis of AdoCbl genes (Rodionov *et al.*, 2003). Despite the low sequence identity, and notable gaps in the sequence of BluE relative to *Se*PduX (residues 105–108, 180–190, and 283–288), the sequence alignment revealed multiple conserved residues. Several of these residues were previously identified as important for *Se*PduX function (Fan & Bobik, 2008, Fan *et al.*, 2009) (Fig. 2). A phylogenetic tree was constructed from *Se*PduX and BluE from *R. sphaeroides* and *R. capsulatus* protein sequences (Fig. 3). We identified two distinct phylogenetic clusters. At the bottom of this tree were closely related homologues of *Se*PduX (green lettering). This cluster contained organisms that synthesized homologues of the cobaltochelatase *Se*CbiK or CbiX (EC 4.99.1.3, red squares) and therefore use the early-cobalt-insertion pathway for AdoCba biosynthesis (Fig. 1A). At the top of the tree is a cluster containing organisms that synthesize BluE homologues (blue lettering). This BluE cluster contained members only from the order *Rhodobacterales*, with one exception, a representative from the *Rhizobiales* (*i.e., Maganema perideroedes*). This cluster was comprised only of organisms that contained all three subunits of the cobaltochelatase CobNST (EC 6.6.1.2, green squares), which is a marker for the late-cobalt-insertion pathway. *Rhodobacterales* are known to use the late-cobalt-insertion pathway [reviewed in (Mattes *et al.*, 2017)]. The one exception in the cluster is a *Roseobacter* species, which oddly possessed genes that encoded two of the three subunits of the late-Co-insertion pathway cobaltochelatase CobST but not CobN and lacked all the genes of the early *de novo* biosynthetic pathway. It had all the genes for the late steps of the pathway (*cobCDOPUV, bluEF*) and must therefore salvage precursors such as cobyric acid (Cby) or cobinamide (Cbi) (Fig. 1B) in order to assemble the nucleotide loop and produce AdoCbl. The *Rhodobacterales* that encoded BluE also encoded the 5,6-dimethylbenzimidazole (DMB) synthase, BluB (EC 1.14.99.40, purple squares) (Gray & Escalante-Semerena, 2007, Taga *et al.*, 2007). Possible implications of this genetic affiliation are discussed below.

R. capsulatus and *R. sphaeroides* BluE restore AdoCbl-dependent growth of a *S. enterica* Δ*pduX* strain.

S. enterica encodes two methionine synthases, the Cba-dependent (MetH, EC 2.1.1.13) (Drennan *et al.*, 1994, Bandarian *et al.*, 2002) and the Cba-independent methionine synthase (MetE, 2.1.1.14) (Pearlso *et al.*, 2001, Gonzalez *et al.*, 1992, Hondorp & Matthews, 2004), both of which synthesize methionine from homocysteine and methyl-tetrahydrofolate. The Cba-dependent MetH enzyme has a 57-fold greater enzymatic efficiency than MetE (Taylor & Weissbach, 1973, Jakubowski, 1990), so picomolar concentrations of Cba is sufficient to meet the methionine synthesis needs of *S. enterica* under laboratory conditions (Bradbeer, 1982). We used a *S. enterica* Δ*metE* Δ*pduX* mutant strain to show *in vivo* that BluE had L-Thr kinase function. It has been observed by us and others (Fan & Bobik, 2008) that when a

S. enterica Δ*metE* Δ*pduX* strain is grown on minimal glycerol medium with relatively high levels of exogenous Cby (*i.e.*, >5 nM), the strain does not display a robust growth phenotype relative to the wild-type strain. One reason for this was the very low levels of Cba required by the Cba-dependent methionine synthase (MetH) (Andersson & Roth, 1989). The results also suggested the presence of at least one other enzyme with L-Thr kinase activity within *S. enterica*. This hypothetical, redundant kinase activity only restored AdoCba synthesis in a Δ*pduX* mutant strain when the intracellular levels of Cby were high. For this reason, growth analysis was performed with a low Cby concentration (1 nM) to clearly distinguish the Δ*pduX* growth phenotype when assaying MetH Cba-dependent growth. Likewise, when cells were grown under conditions that demanded a much higher level of AdoCba production, such as growth with ethanolamine as the sole carbon and energy source (Roof & Roth, 1988, Roof & Roth, 1989), a *S. enterica* Δ*pduX* mutant strain did not grow (Fig. 4A, open circles) (Fan & Bobik, 2008).

Figure 4 shows the growth behavior of *S. enterica* Δ*pduX* mutant strains expressing genes from plasmids encoding *R. sphaeroides* locus RSP_0788 (p*Rs*BluE, open squares), *R. capsulatus* locus RCAP_rcc02055 (p*Rc*BluE, closed squares), *S. enterica pduX*$^{+}$ (p*Se*PduX, closed triangles), and the corresponding vector-only controls. The culture medium contained ethanolamine (90 mM) as the carbon and energy source supplemented with cobalamin precursors Cby (300 nM) or Cbi (300 nM) and DMB (0.15 mM). Aerobic growth on ethanolamine requires a high concentration of Cba or corrinoid Cba precursors (*e.g.* Cby or Cbi) (Roof & Roth, 1988, Roof & Roth, 1989) and base (*e.g.* DMB or adenine) to keep up with the AdoCba demand necessary to utilize this carbon and energy source (Anderson *et al.*, 2008). The use of Cby allowed us to probe the AP-P synthesis branch directly, while using Cbi functions as a positive control by bypassing the AP-P linker synthesis and attachment branch (Fig. 1). *Rc*BluE restored AdoCba biosynthesis in the *S. enterica* Δ*pduX* strain allowing the culture to reach the same cell density as that of the cultures of wildtype *S. enterica pduX*$^{+}$. Expression of *S. enterica pduX*$^{+}$ (p*Se*PduX, closed triangles) improved growth over that of the wild-type *pduX*$^{+}$ strain (open triangles) whether or not the chromosomal *pduX*$^{+}$ gene was deleted (closed triangles *vs* closed circles); the strains grew with similar doubling times (*i.e.*, 3.7 h) (Fig. 4A, closed circles and triangles). However, cultures of strains producing *Rs*BluE or *Se*PduX displayed a much shorter lag time (12 and 16 h, respectively) than cultures of the wild-type strain carrying the empty cloning vector, or the strain producing *Rc*BluE (*i.e.*, 26 h) (Fig. 4A, closed squares). *Rs*BluE restored AdoCba synthesis in a Δ*pduX* strain with roughly the same doubling time (*i.e.*, 2.7 h) as *Se*PduX (Fig. 4A, open squares *vs* closed triangles). Figure 4B shows the effect of adding the Cba precursor Cbi, which enters the pathway downstream of the enzymes that synthesize and attach the AP-P linker moiety (Fig. 1B). As expected all the strains grew like wildtype, except for a slightly longer lag time for the Δ*pduX*/p*Rc*BluE strain. These results showed that BluE from *R. sphaeroides* or *R. capsulatus* efficiently substituted for PduX in *S. enterica*. Using sequence alignments of *Se*PduX and BluE homologues (Fig. 2), we targeted conserved residues for substitution. Expression of a *R. sphaeroides bluE* allele encoding variant *Rs*BluE^{G99A}, failed to restore AdoCba biosynthesis in a *S. enterica* Δ*pduX* strain under conditions that demanded either low (Fig. S1A) or high (Fig. S1B) AdoCba levels for growth. Figure 5 shows the effect of the *Rs*BluE^{G99A} variant on Cba-dependent growth of *S.*

enterica when precursors for each enzyme in the AP-P synthesis and attachment branch of the Cba biosynthesis pathway was provided exogenously. As expected, when L-Thr was provided to a Δ*pduX* strain producing the *Rs*BluE^{G99A} variant it failed to grow (Fig. 5A, closed diamonds), but grew well in a wild-type *pduX*$^{+}$ strain background (open diamonds), presumably because the presence of the native wild-type *Se*PduX enzyme produced from the chromosomal copy of the gene compensated for the presence of the defective *Rs*BluE^{G99A} enzyme produced from a plasmid. Surprisingly, when the product of *Se*PduX/*Rs*BluE and substrate of *Se*CobD (L-Thr decarboxylase), L-Thr-P, was provided to bypass the L-Thr kinase function, the Δ*pduX*/p*Rs*BluE^{G99A} strain was still unable to grow (Fig. 5B). Likewise, when ethanolamine phosphate (EA-P), the product of *Se*CobD and substrate of *Se*CbiB (AdoCbi-P synthase) was provided the Δ*pduX*/p*Rs*BluE^{G99A} strain was still unable to grow. *Se*CbiB was previously shown to use EA-P as a Cba linker in *S. enterica* to generate nor-Cbas (Zayas *et al.*, 2007). Only when the entire linker synthesis and attachment branch is bypassed (Fig. 1) by the addition of Cbi (Fig. 5D) was the Δ*pduX*/p*Rs*BluE^{G99A} strain able to grow. The implication of these results are discussed below.

Inactivation of *bluE* in *R. sphaeroides* causes AdoCbl-dependent growth phenotypes.

Since the presence of *Rs*BluE restored growth of a *S. enterica* Δ*pduX* strain under AdoCbl dependent growth conditions (Fig. 4, 5, S1), the function of this gene was assessed in *R. sphaeroides*. *R. sphaeroides* cells grown aerobically with acetate (30 mM) as the sole source of carbon and energy. *R. sphaeroides* uses a Cbl-dependent ethylmalonyl-CoA mutase (Erb *et al.*, 2008) and methylmalonyl-CoA (Banerjee, 2003) mutase to catabolize short chain fatty acids such as acetate (Gray & Escalante-Semerena, 2009b, Banerjee, 2003). When no cobamide precursors were added to the medium, Δ*bluE* strains failed to grow compared to *bluE*$^{+}$ controls (Fig. 6A, asterisks *vs* circles). We also observed a “blush” phenotype for the Δ*bluE* strain and noted that the amount of light-harvesting complex 1 (LH1 B875) reaction center pigments of this strain were reduced relative to those in cultures of the Δ*bluE* strain growing in the presence of AdoCbl (Fig. S2A,B) after measurements were normalized for the cell density of each culture. The blush phenotype was also corrected by the addition of CNCbl to the medium (Fig. S2C)

To further validate BluE as a L-Thr kinase, we used a *R. sphaeroides* Δ*cobB* strain, which could not synthesize adenosylcobyric acid (AdoCby) *de novo* under the aerobic conditions tested because of the disruption of the early steps O_2-depenent (late-Co-insertion) pathway (Fig. 1A). AdoCba biosynthesis in the Δ*cobB* strain was restored by feeding Cby, the substrate for the adenosylcobinamide-phosphate (AdoCbi-P) synthase (CobD; CbiB in the early-Co-insertion pathway) enzyme (Fig. 6, pathway scheme). As expected, *R. sphaeroides* Δ*cobB* Δ*bluE* mutants did not grow in medium containing Cby, unless *bluE*$^{+}$ was provided on a plasmid (Fig. 6B, triangles). Although growth of the Δ*bluE*/p*Rs*BluE strain was delayed, the doubling time (6 h) and final density (OD_{630} = 0.6) of the culture was similar to that of the *cobB*$^{+}$ *bluE*$^{+}$ strain (4 h, OD_{630} = 0.6; Fig. 6B, circles *vs* squares). Even when the AP-P synthesis branch of the pathway is bypassed by the addition of the Cbl precursor Cbi (Fig. 6, pathway scheme) to the medium, all mutant strains displayed a slight delay in the onset of exponential growth relative to the *cobB*$^{+}$ *bluE*$^{+}$ (Fig. 6C). What this might indicate

about the physiology of Cba biosynthesis in this organism is discussed below. Collectively, results shown in figure 6 validated BluE as a *bona fide* L-Thr kinase in *R. sphaeroides*.

Enrichment of *Rs*BluE and *Se*PduX.

Overproduction of *Rs*BluE and *Se*PduX resulted, in both cases, in the production of substantial quantities (~12 mg g^{-1} cells) of insoluble protein. Several strains of *E. coli* overexpression strains (BL21, BL21/RIL, Rosetta 2/plysS, BL21/plysSRARE2, C41, C43, MDS 42, and Lemo21), and *S. enterica* at various temperatures (15, 25, 37°C), with different lysis methods (chemical lysis, French press, and sonication), buffers (HEPES, Tris-HCl), pH (7.0, 7.5, 7.9, 8.0, and 8.5), under normoxic and anoxic conditions were tried with little success at improving the quantity of soluble protein isolated. Tags used to increase protein solubility such as maltose binding protein (MBP) resulted in an inability to detect protein production either due to poor expression or proteolysis prior to cell harvesting. Several different detergents were screened in an attempt to solubilize proteins. Detergents used included 3-[(3-cholamidopropyl)dimethylammonio]-1-propanesulfonate (CHAPS), *n*-dodecyl-β-*D*-maltopyranoside (DDM), Fos-choline-16 (FOS16), Triton-X, sarkosyl, and sodium dodecyl sulfate (SDS). The proteins were only soluble in SDS or sarkosyl. Attempts to completely remove the detergent after solubilization resulted in protein precipitation. A concentration of ~1% (w/v) sarkosyl was maintained to keep the proteins in solution. *N*-terminally His_6-tagged protein was overproduced, solubilized, and purified to 70% purity with the detergent sarkosyl as described in the *Experimental procedures* section. The sarkosyl concentration was reduced to ~1% (w/v) by dialysis. Figure 7A shows a representative SDS-PAGE gel of purified *Rs*BluE and *Se*PduX. Both enzymes were active in the presence of ~1% (w/v) sarkosyl. Proteins isolated in this manner were used for all *in vitro* assessment of ATPase activity using the ADP-Glo™ ATPase Assay kit described under *Materials & Methods*.

*Rs*BluE has ATPase and L-Thr kinase activities *in vitro*.

Figure 7B shows representative results of an ATP activity assay using the ADP-Glo™ Assay kit. Sarkosyl-solubilized *Rs*BluE and *Se*PduX (12 μM) exhibited ATPase activity when provided with ATP (0.1 mM) and L-Thr (10 mM). ATP to ADP conversion was quantified by comparison to a standard curve (Fig. S3). *Se*PduX converted 99% of the ATP to ADP, *Rs*BluE converted 61%, and the $RsBluE^{G99A}$ variant converted 21% after 1 h incubation at 25°C. There was residual 8% ATPase activity detected in the reaction with extracts from the vector control. With L-Ser as the substrate, *Se*PduX converted 90% of the ATP to ADP, *Rs*BluE converted 51%, and the $RsBluE^{G99A}$ variant converted 30%. There was no activity detected in the reactions with extracts from the vector control. These data implied that sarkosyl-solubilized *Se*PduX was a more efficient enzyme than *Rs*BluE *in vitro* under the conditions tested. These data also suggested that *Se*PduX and *Rs*BluE might be able to use L-Ser as substrate to generate *O*-phospho-L-serine (L-Ser-P).

We employed a biological assay to verify the generation of L-Thr-P and L-Ser-P by sarkosyl-solubilized *Rs*BluE. *Rs*BluE reactions were filter sterilized and added to minimal glycerol medium supplemented with Cby used to grow *S. enterica* strains (Fig. 7C, D). *Rs*BluE reactions containing L-Thr and ATP restored near wild-type growth (Fig. 7C, open

circles *vs* triangles) of a Δ*pduX* strain when compared to the same strain grown in medium containing the reactions of extracts from the vector control (Fig. 7C, open circles *vs* diamonds). These results showed that *Rs*BluE had L-Thr kinase activity *in vitro*. A Δ*cobD* strain was included as a negative control since only AP-P, not L-Thr-P, would restore growth of the Δ*cobD* strain (Fig. 7D, diamonds). Figure 7D shows the growth of strains in medium supplemented with reactions containing L-Ser and ATP. The presence of L-Ser from the vector only or *Rs*BluE reactions strongly inhibited growth of Δ*pduX* strains (Fig. 7D, diamonds and circles). The wild-type strain also exhibited an increased lag from 2 to 6 hours but eventually reached full density (Fig. 7D, triangles). These results suggested that L-Ser had a slight inhibitory effect on the growth of *S. enterica*, an effect that was greatly exacerbated in the Δ*pduX* strain. This idea was further explored (see below).

Optimal conditions for the *Rs*BluE *in vitro* activity assay.

The reaction conditions for the L-Thr kinase reaction were optimized (Fig. S8). The optimal pH was 8 in HEPES buffer (50 mM) (Fig. S8A). Sarkosyl-solubilized *Rs*BluE was 57% and 67% more active at low protein concentrations (2 μM) than at 12 and 24 μM protein, respectively (Fig. S8B). However, the total percent conversion after a 1-h incubation period at 25°C was greater at higher concentrations of protein; 81% at 24 μM, 54% at 12 μM, and 20% at 2 μM (data not shown). Salts were not required for activity, and $CaCl_2$ (100 mM) decreased the activity of the enzyme by 75% (Fig. S8C). However, a divalent metal ion (1 mM) was required for *Rs*BluE ATPase activity, with optimal activity observed with $MnCl_2$. *Rs*BluE used $MgCl_2$, $ZnCl_2$, $NiCl_2$, and $CaCl_2$ equally well. $CoCl_2$ did not support the ATPase activity of *Rs*BluE as well as the other metals but did perform better than the no metal control (Fig. S8D). The concentration of L-Thr did not affect the ATPase activity for *Rs*BluE. There was a slight drop in activity at 50 and 100 mM L-Thr concentration (Fig. S8E) and increasing the concentration of L-Ser inhibited *Rs*BluE ATPase activity (Fig. S8F). *Rs*BluE hydrolyzed ATP in the absence of L-Thr, and in the presence of L-Ser, D-Ser, D-Thr, L-Tyr, or L-Val (10 mM), without only slightly higher activity levels for L-Ser, D-Ser, and D-Thr relative to the ATP only control and L-Tyr and L-Val had similar activity levels to that of the ATP only control (Fig. S8G). *Rs*BluE ATPase activity is independent of potential amino acid substrate. Figure S8H shows the activity of *Rs*BluE as a function of ATP concentration. *Rs*BluE activity ATP activity increased with increasing ATP concentration (1–20 mM) as was observed in figure S7A. *Rs*BluE was assayed for inhibition by known ATPase inhibitors (Fig. S8I). ADP was the most effective inhibitor followed by pyrophosphate (PPi), with a 52% and 12% decrease in activity, respectively. Surprisingly, *ortho*-phosphate (Pi) and adenosine 5′-[γ-thio]triphosphate (ADP-γ-S) increased the activity of *Rs*BluE by 8% and 22%, respectively. It may be possible that *Rs*BluE can hydrolyze ADP-γ-S. There are precedents of enzymes using ADP-γ-S. as substrate (Smith *et al.*, 2011). Further testing of *Rs*BluE with ADP-γ-S will be needed. The inhibition of *Rs*BluE by one of its products, ADP, could have implications for how this enzyme is regulated.

Detergent-free *Rs*BluE and *Se*PduX can be isolated in low concentrations.

While the sarkosyl-solubilized proteins displayed robust ATPase activity *in vitro*, and kinase activity using a sensitive biological assay (Fig. 7C), we did not detect L-Thr kinase activity

using ^{31}P-NMR spectroscopy. The implication being that sthe sarkosyl-solubilized protein had kinase activity that was present but reduced or impaired. The mechanism of sarkosyl solubilization of proteins is generally achieved by the partial unfolding of proteins. While this did not appear to affect the ATPase activity of *Rs*BluE, it did have an effect on the transfer of the phosphoryl moiety to L-Thr. For this reason, we attempted to purify *Rs*BluE and *Se*PduX without the aid of detergents. While most of produced protein was insoluble, small quantities of His_6-tagged protein bound to a Ni-NTA affinity chromatography resin and were eluted with imidazole (200 mM). Notably, these proteins were only soluble for < 60 min before precipitating. Neither temperature (4, 25°C), dialysis to remove imidazole, or the addition of glycerol improved protein stability. *Rs*BluE and *Se*PduX were purified to a purity of 87% and 89% respectively (see Experimental procedures). This window of protein stability afforded the opportunity to assess protein function without detergent. Extracts from cells carrying the empty vector pTEV5 were isolated in an identical manner and fractions eluted at the same imidazole concentration (200 mM) were collected and used as negative controls (Fig. S4). Proteins isolated in this manner were used to assay the generation of L-Thr-P by ^{31}P-NMR spectroscopy. Concerns about possible interference by the *N*-terminal His_6-tag lead us to test the solubility and purification of previously published non-cleavable *C*- and *N*-terminally tagged *Se*PduX proteins (Fan *et al.*, 2009, Fan & Bobik, 2008). *Se*PduX exhibited the same poor solubility regardless of the placement or cleavability of the His_6- or His_8-tag. The majority of the protein was found in the insoluble fraction and only small amounts of limited stability protein was isolated (Fig. S5).

*Rs*BluE generates L-Thr-P *in vitro*.

We used ^{31}P-NMR spectroscopy to confirm that *Rs*BluE transferred a phosphate from ATP to L-Thr to generate L-Thr-P; figure 8 shows representative ^{31}P-NMR spectra. Panel A shows the spectrum for standards of polytriphosphate (PPPi), pyrophosphate (PPi), and *ortho*-phosphate. Panel B shows the spectrum of the reaction mixture without enzyme but containing ATP and L-Thr-P. Enzymatic reactions containing ATP and *Rs*BluE (panel C), ATP, L-Thr, and *Rs*BluE (panel D), and ATP, L-Thr, and extracts from cells carrying the pTEV5 empty vector (panel E). For those experiments we used detergent-free protein extracts obtained as described above and in *Experimental prodecures*. As a result, some conversion of ATP to ADP and free phosphate (Pi) and pyrophosphate (PPi) was observed, likely due to contaminating proteins with ATP/ADP hydrolysis activities. This was confirmed by the presence of signals with chemical shifts corresponding to PPi (6.1 ppm) and Pi (2.9 ppm) in the reactions containing extracts from cells expressing the empty vector pTEV5, which was included as a negative control (Fig. 8E). When *Rs*BluE was incubated with ATP and L-Thr a signal with a chemical shift of 3.6 ppm corresponding to authentic L-Thr-P was detected (Fig. 8D). This signal was absent in the spectrum of reaction mixtures containing only *Rs*BluE and ATP (Fig. 8C), or cell-free extracts of cells carrying the empty pTEV5 vector (Fig. 8E). These results supported the idea that *Rs*BluE was a *bona fide* L-Thr kinase. GTP was also tested as a phosphor donor and failed to generate GDP or L-Thr-P (data not shown), indicating *Rs*BluE could not use GTP as a phosphoryl donor. *Se*PduX was previously shown to have very low levels of activity with GTP, CTP, or UTP and a strong preference for ATP (Fan & Bobik, 2008).

L-Ser inhibits a *S. enterica* Δ*pduX* strain *in vivo*.

To address the L-Ser inhibition shown in figure 7D (diamonds and circles), we grew *S. enterica* strains in minimal glycerol + Cby medium supplemented with either L-Thr, L-Thr-P, L-Ser, or L-Ser-P (Fig. 9). The addition of L-Thr-P improved the growth rates and cell yields of the *pduX*$^+$ and Δ*pduX* strains (red squares, cyan circles; overlapping) over those of the *pduX*$^+$ strain with no supplements (open circles). L-Thr also improved the growth behavior of wildtype (*pduX*$^+$, black circles) and Δ*pduX* strains (black squares) to a slightly lesser extent than L-Thr-P. These results suggested that exogenous L-Thr was used by PduX. Notably, the Δ*pduX* strain grew well in the absence of L-Thr or L-Thr-P (Fig. 9, open squares). Possible explanations for the growth behavior of the Δ*pduX* strain are discussed below.

As shown in figure 7D, the addition of L-Ser caused a slight increase in the lag time of the wild-type strain compared to the addition of L-Thr (Fig. 7C), and strongly inhibited growth of a Δ*pduX* strain (Fig. 7D, diamonds), even when expressing *pduX*$^+$ from a plasmid (Fig. 7D, circles). The addition of L-Ser-P did not affect the growth of the *S. enterica pduX*$^+$ strain (Fig. 9B, blue circles *vs* open circles), or Δ*pduX* strain (Fig. 9B, red squares *vs* open squares). As expected, the addition of L-Thr-P or L-Ser-P did not affect the growth behavior of the Δ*cobD* strain (Fig. 9A, 9B solid triangles), which requires AP-P for growth.

To further validate the above *in vivo* results, we performed ^{31}P-NMR analyses of the *Rs*BluE reaction mixtures containing ATP and L-Ser (Fig. S6). *Rs*BluE did not synthesize L-Ser-P from ATP and L-Ser (Fig. S6C).

*Se*PduX and *Rs*BluE use L-Thr more efficiently than L-Ser, and ATP is the limiting substrate.

We measured the specific activity of sarkosyl-solubilized *Se*PduX and *Rs*BluE using a pyruvate kinase/lactate dehydrogenase coupled assay that indirectly measured the generation of ADP via the consumption of NADH (see Experimental procedures) (Bergmeyer *et al.*, 1985) (Fig. S7). Shown in figure S7 are the specific activities of *Rs*BluE (Fig. S7A) and *Se*PduX (Fig. S7B) as a function of ATP, L-Thr (Figs. S7C, D), and L-Ser (Figs. S7E, F). The concentration of L-Thr was held constant at 50 mM as the ATP concentration was increased, and *vice versa*, the ATP concentration was held at 50 mM while L-Thr or L-Ser concentrations were increased. *Se*PduX and *Rs*BluE had comparable specific activities for ATP, that is, 1.0 and 0.93 μmol ATP per minute per mg of protein (Table 1). However, complete substrate saturation was not reached. The rate of ATP hydrolysis did not change as a function of the concentration of L-Thr (Fig. S7C, S7D). Even when no L-Thr was present in the reaction mixture, both enzymes hydrolyzed ATP to ADP. This is also illustrated in figure S8G. *Se*PduX specific activity declined by 9% when L-Thr was the substrate and 35% when L-Ser was used, resulting in a 29% difference in activity between L-Thr and L-Ser as substrates. The effect was more severe for *Rs*BluE, with a 17% decline in activity when L-Thr was present and 55% with L-Ser, for a 46% difference in specific activity between L-Thr and L-Ser as substrates. This decrease in *Rs*BluE activity in the presence of increasing L-Ser concentration is illustrated graphically by the gradual downward slope of the curve in figures S7E and S8F in contrast to the relatively flat line for the *Rs*BluE reactions with L-

Thr (Figs. S7C and S8E), or the *Se*PduX reaction with L-Ser (Fig. S7F). This result suggested an inhibitory effect by L-Ser on *Rs*BluE.

Discussion

The *bluE* genes of *R. capsulatus* and *R. sphaeroides* encode L-Thr kinases.

In vivo (Fig. 4, 6) and *in vitro* (Fig. 8) data provide strong support to our assignment of function to BluE proteins from *R. capsulatus* (*Rc*BluE) and *R. sphaeroides* (*Rs*BluE) as L-Thr kinases that synthesize L-Thr-*O*-3-phosphate (L-Thr-P). Although some differences between *Rc*BluE and *Rs*BluE were observed during their *in vivo* function analysis (Fig. 4), those differences may be due to several factors. We can only speculate about the possibilities, such as structural differences in *Rc*BluE that prevent optimal interaction with native *S. enterica* proteins in the pathway. This might explain why the Δ*pduX* / p*Rc*BluE strain had a slightly longer lag time when grown on media supplement with Cbi (Fig. 5B), a condition which bypasses the need for BluE or PduX (Fig. 1B). *Rc*BluE may be simply a less catalytically efficient enzyme. At the moment insufficient information is available to compare catalytic effciencies.

Rhodobacterales may have evolved *Rs*BluE to avoid synthesizing nor-Cbl.

Our data (Figs. S5, S6) support the idea that *Rhodobacter sphaeroides* and probably other *Rhodobacterales* that possess the BluE enzyme may have a preference or requirement for Cbl, that is, the Cba that has AP-P, not EA-P, as the nucleotide linker. The restriction against the synthesis of norCbas with EA-P as the linker derived from L-Ser-P, was made clear by the results of *in vitro* experiments (Fig. 7B, S6, S5, S7F). Based on those data we suggest that the L-Thr-P decarboxylase (CobC; CobD in the early-Co-insertion pathway) (Fig.1) in these bacteria likely also have a strong preference for L-Thr-P, given that growth was poorly supported by L-Ser-P relative to the response to L-Thr-P (Fig. 9). The catalytic activities of Cba-dependent enzymes from these bacteria must be analyzed to gain insights into the specificity of the enzymes for Cbl. While the data presented here suggests that *Rhodobacterales* prefer Cbl, other than the inability of *R. sphaeroides* to use pseudo-Cbl (Gray & Escalante-Semerena, 2009a), the ability of all other *Rhodobacterales* that synthesize BluE to use other form of Cbas has not been tested. At this time the Cba preference of these *Rhodobacterales* remains speculative.

Phylogenetic analyses suggest that BluE is not the L-Thr kinase of the late-cobalt-insertion pathway.

At first glance, it appears that BluE is found exclusively in organisms that synthesize the CobNST cobaltochelatase of the late-cobalt-insertion pathway (Fig. 3). BLASTP searches using *Se*PduX retrieved homologues only from organisms that use the early-cobalt-insertion pathway. The only exception being *T. lienii*, which lacks all the genes of the early corrinoid biosynthesis pathway. BluE appears to be restricted only to the order *Rhodobacterales* and is not found in any other group that uses the late- or early-cobalt-insertion pathway.

The BluE protein is the L-Thr kinase of a subgroup of *Rhodobacterales* with a preference for AdoCbas with AP-P as the nucleotide linker and DMB as the ribotide base.

While BluE is present in *R. sphaeroides* and *R. capsulatus* it is not found in other AdoCba producing purple photosynthetic bacteria such as *Rhodopseudomonas palustris* (Order *Rhizobiales*) or *Rhodospirillum rubrum* (Order *Rhodospirillales*). In addition, BluE is not found in *Rhodobacterales* such as *Silicibacter pomeroyi, Dinoroseobacter shibae, Ruegeria pomeroyi*, and *Jannashia*. Homologues of PduX or BluE have not been identified in these other purple photosynthetic bacteria or in archaea, leaving open the question of how these organisms produce L-Thr-P. Recent work identifying a bifunctional version of CobD in *M. Mazei* that has both L-Thr decarboxylase and L-Thr kinase activities might offer a clue (Tavares *et al.*, 2018). It is not clear what evolutionary or metabolic distinction may be responsible for the restriction of BluE to this small group of *Rhodobacterales*.

Importantly, *Rhodobacterales* that possess BluE also encode the 5,6-dimethylbenzimidazole (DMB) synthase, BluB (EC:1.13.11.79) (Gray & Escalante-Semerena, 2007, Taga *et al.*, 2007) (Fig. 3). Organisms that encode BluB appear to have a strong preference for DMB as the lower ligand base and do not synthesize or use Cbas with other bases (Taga *et al.*, 2007, Gray & Escalante-Semerena, 2007, Campbell *et al.*, 2006). Several of these *Rhodobacterales* also encode CbiZ, an amidohydrolase (EC 3.5.1.90) known to cleave AdoCbas between the secondary amine of the (*R*)-1-aminopropan-2-ol (AP) moiety that links the nucleotide to an ester on the corrinoid ring to form the nucleotide loop (Gray & Escalante-Semerena, 2009a). CbiZ from *R. sphaeroides* has been shown to cleave nucleotide loops that do not have DMB as the base, such as Adopseudo-Cbl, which has adenine as the base, or to a lesser extent, AdoCbi, which only has the AP moiety without a nucleotide attached (Gray & Escalante-Semerena, 2009a). The activity of CbiZ allows cobyric acid (Cby, the product of the CbiZ reaction) (Fig. 1) to re-enter the biosynthetic pathway thereby allowing *R. sphaeroides* to remodel salvaged Cbas by incorporating the preferred DMB base into the final product (Woodson & Escalante-Semerena, 2004, Gray & Escalante-Semerena, 2009b, Gray & Escalante-Semerena, 2009a). The presence of both BluE and BluB in these *Rhodobacterales* could imply a preference for the Cba with DMB as the base and AP-P as the nucleotide linker, known as adenosylcobalamin (AdoCbl, *Coα*-(α−5,6-dimethylbenzimidazolyl-*Coβ*-adenosylcobamide).

The genetic makeup of these *Rhodobacterales* led us to speculate about the evolutionary and or environmental context for the presence of these particular sets of genes. The Cbl-dependent ethylmalonyl-CoA mutase and methylmalonyl-CoA mutase enzymes in these organisms may require Cbl for optimal functionally and may not be as enzymatically active with other Cbas such as norCbas (EA-P as the linker rather than AP-P) or Cbas with lower ligands bases other than DMB, such as pseudo-Cbl (adenine as the base). To our knowledge the enzymatic activity of these enzymes with different Cba cofactors has not been reported.

In the environmental context, pseudo-Cbl is the dominant corrinoid found in marine surface water. While pseudo-Cbl is produced by other prokaryotes, cyanobacteria are thought to be the primary producer of pseudo-Cbl in marine environments. *Thaumarchaeota* (early-Co-insertion pathway) and *Rhodobacterales* (late-Co-insertion pathway) are thought to be the primary producers of Cbl (Cbas with DMB as the base) in marine environments (Heal *et al.*,

2017, Doxey *et al.*, 2015). Norpsuedo-Cbl has not been directly measured in marine waters but organohalide respiring bacteria that possess genes for norpseudo-Cbl dependent reductive dehalogenase (Kräutler *et al.*, 2003) are known to inhabit marine subsurface sediments (Futagami *et al.*, 2009) and have association with marine sponges (Liu *et al.*, 2017). Eukaryotes cannot synthesize Cbas and must rely on dietary sources or symbiotic relationships with bacteria to acquire it. Eukaryotes can only take up and use Cbl and do use other Cbas such as pseudo-Cbl or norpseudo-Cbl. Some *Rhodobacterales* have symbiotic associations with marine phytoplankton (Amin *et al.*, 2012, Buchan *et al.*, 2014), that appear to obtain AdoCbl from their bacterial symbionts (Croft *et al.*, 2005, Croft *et al.*, 2006). The presence of *cbiZ* in the genomes of many *Rhodobacterales* confers an advantage to these microorganisms by allowing them to salvage pseudo-Cbl, which is the dominant marine species of Cbas, and potentially norpseudo-Cbl, and remodel them into Cbl, their preferred Cba. CbiZ activity has not been tested against norCbas, so its ability to cleave norpseudo-Cbl is unknown. The enzymatic preference towards producing only AdoCbl may be a result of evolutionary pressure on some *Rhodobacterales* in symbiotic relationships to produce only AdoCbl to accommodate their eukaryotic host's specific metabolic requirements.

In vivo BluE phenotypes revel potential protein-protein interactions indicative of Cba biosynthesis enzyme complex.

It was surprising that the absence of an enzyme like CobB, which is involved in the early steps of the corrinoid ring biosynthesis pathway had impaired growth (Fig. 6C) when that portion of the pathway was bypassed by the addition of Cbi (Fig. 1B, Fig. 6, pathway scheme). One explanation for this result is CobB and possibly other proteins in the early steps of the pathway may interact with proteins in the late steps of the pathway such as CobD (CbiB in the early-Co-insertion pathway), in a Cba biosynthetic protein complex. Removal of either CobB (Fig. 6C, open squares) or BluE (asterisks) disrupts the protein complex and is further exacerbated by the removal of both (closed triangles). This would explain why the Δ*cobB* Δ*bluE*/p*Rs*BluE strain had delayed growth (Fig. 6B, open squares *vs* Fig. 6A open diamonds), because while the enzymatic activity of CobB is not required, the presence of the protein itself may be required to stabilize a protein complex. These results are similar to the growth behavior of the *Rs*BluE^{G99A} variant in *S. enterica* (Fig. 5). Cumulatively, the results in figure 5 showed in *S. enterica* that only when the entire AP-P linker synthesis and attachment branch of the Cba synthesis pathway was bypassed by the addition of Cbi (Fig. 5D) was the Δ*pduX*/p*Rs*BluE^{G99A} strain able to grow. These results obtained with *S. enterica* suggest that in *R. sphaeroides* the *Rs*BluE protein not only interacts with protein of the early steps like CobB but also with the L-Thr-P decarboxylase (CobD/CobC) and the AdoCby-P synthase (CbiB/CobD) enzymes. We speculate that this may occur through the formation of a multiprotein biosynthetic complex anchored to the membrane by the transmembrane AdoCby-P synthase (CbiB/CobD) protein (Zayas *et al.*, 2007). Evidence supporting the idea of a Cba biosynthetic protein complex has been previously presented by our lab and others (Raux *et al.*, 1996, O'Toole *et al.*, 1993).

Conclusions

*Se*PduX was the first enzyme reported to phosphorylate free L-Thr (Fan & Bobik, 2008), and it is annotated as a member of the GHMP kinase family (Bork *et al.*, 1993). Here we add BluE from the *Rhodobacterales* as a new member of that family. Further investigation of BluE may reveal mechanistic differences with *Se*PduX. There are several gaps in the late-cobalt-insertion AdoCba biosynthesis pathway, and within AdoCbl producers like *R. sphaeroides*, which appear to have a strong preference for the Cbas they synthesize and use. We have identified BluE as the L-Thr kinase for some of these *Rhodobacterales*. How other organisms that do not possess *bluE* or *pduX* generate L-Thr-P or L-Ser-P remains an open question.

Experimental procedures

Phylogenetic analysis and tree construction.

Sequences were obtained using Basic Local Alignment Search Tool for Protein (BLASTP) (Altschul *et al.*, 1997). The protein sequences of the following proteins were used to search for homologues in the Integrated Microbial Genome (IMG) database (Markowitz *et al.*, 2006). *Rs*BluE (RSP_0788), *Rc*BluE (RCAP_rcc02055), *Se*PduX (STM2058), *Se*CbiK (STM2025), *Rs*BluB (RSP_3218), *Rs*CobN (RSP_2827), *Rs*CobS (RSP_1977), *Rs*CobT (RSP_1976) *Dh*CbiX (DeshaDRAFT_4176) from *Desulfitobacterium hafniense* Y51, and *Bm*CbiX (BMQ_2618) from *Bacillus megaterium* QM B1551. Only finished or permanent draft genomes with bit scores > 50 or *e* values > $1.0e^{-7}$ and *pduX* homologues adjacent to Cba biosynthetic or utilization genes on the chromosome were used in the analysis. The *bluE* homologues identified were always associates with Cba genes on the chromosomes. Locus tags and phylogenetic information for PduX and BluE homologues used to construct the phylogenic tree are listed in Table S3. Sequence header files were simplified with the find/replace and *grep* functions of TextWrangler (Bare Bones Software). Outliers and sequences with extreme divergence were not included nor were alleles not associated with AdoCba biosynthetic gene clusters on the chromosome. FASTA formatted sequences were aligned using the MUSCLE (Edgar, 2004) plugin within Geneious R8.1.7 software (Biomatters Ltd.) with 100 iterations and default settings. Phylogenetic trees were constructed with maximum likelihood using the online PhyML (Guindon *et al.*, 2010) tool on the ATCG Montpellier Bioinformatics Platform (http://www.atgc-montpellier.fr/phyml/) using Jones-Taylor-Thornton substitution model (Jones *et al.*, 1992) with 500 bootstrap replicates. The resulting tree was edited using Figtree (Rambaut, 2007) and Illustrator CS6 (Adobe). We used the packages *ape* (Paradis *et al.*, 2004), *geiger* (Harmon *et al.*, 2008), and *diversitree* (FitzJohn, 2012) of the R program (R Core Development Team, 2015) to represent in the phylogeny the presence or absence of CbiK, CbiX, CobNST, or BluB within the genome of each species. We plotted the presence/absence data in the phylogeny using the function *trait.plot* of the *diversitree* (FitzJohn, 2012) package. The presence of CbiK or CbiX homologues are represented as blue boxes on Fig. 3 All three subunits of CobNST had to be present on the chromosome for an organism to receive a green box on Fig. 3, denoting the presence of the complete cobaltochelatase of the late-Co-insertion pathway. ESPript 3.0 (Gouet *et al.*, 1999) was used to generate an image of the alignment. Locus tags of *bluE* and

pduX homologues used in the phylogenetic analysis are available in the *Supplemental Information* section (Table S1).

Bacterial strains and growth conditions.

The genotypes of strains used in this work are described in Table S2. All *S. enterica* strains carried a deletion of the chromosomal copy of the *metE* gene that encodes the AdoCbl-independent methionine synthase (MetE) enzyme (Pearlso *et al.*, 2001). The absence of MetE demands that the cell uses the Cba-dependent methionine synthase (MetH) enzyme to methylate homocysteine (Drennan *et al.*, 1994, Hall *et al.*, 2001, Taylor & Weissbach, 1973). All *S. enterica* strains used in this work also carried a mutation in the arabinose operon (allele *ara-9*) that prevented the utilization of L-(+)-arabinose as a carbon and energy source. Deletions of the Δ*metE* and Δ*pduX* genes in *S. enterica* were constructed using the phage lambda Red recombinase system as described elsewhere (Datsenko & Wanner, 2000).

All *Rhodobacter* strains were derivatives of *Rhodobacter sphaeroides* 2.4.1. *R. sphaeroides* was grown at 30 °C in Sistrom's medium A (Sistrom, 1960) lacking aspartate and glutamate and supplemented with $CoCl_2$ (1 mg L^{-1}). Succinate (10 mM) or acetate (30 mM) were used as sole carbon sources.

Rhodobacter strains construction.

R. sphaeroides genes were inactivated using published protocols (Gray & Escalante-Semerena, 2009b). Primers (Table S3) were used to amplify ~1,500-bp fragments upstream and downstream of the gene of interest. Fragments were fused using overlap extension PCR and cloned into EcoRI and XbaI restriction sites of pK18mobsacB as described below under *Plasmid construction* to generate plasmid pRsBLUE9. The pRsBLUE9 deletion plasmid was transformed into *E. coli* S17-λ cells, which contained conjugal transfer functions for bi-parental mating. *R. sphaeroides* cells were inoculated into 5 mL of Sistrom's medium A containing succinate (10 mM) for 48 h. Cells of *E. coli* strains carrying deletion constructs were inoculated into lysogeny broth (LB) (Bertani, 1951, Bertani, 2004) with kanamycin (0.05 mg mL^{-1}) overnight and sub-cultured (20 % v/v) into LB with no antibiotic the next morning. After 2.5 h of sub-cultured *E. coli* growth, recipient *R. sphaeroides* cells (1.5 mL) were harvested by centrifugation at 6,000 x *g* for 5 min, after which 0.5 mL of a culture of *E. coli* donor strain was added to the tube containing *R. sphaeroides* cells and centrifuged again at 6,000 x *g* for 5 min. Cells were washed with Sistrom's medium (1 mL), pelleted (6,000 x *g*, for 5 min) and re-suspended in 0.1 mL of Sistrom's medium. Cells were plated as a single droplet onto a LB agar plate and incubated for 24 h. Conjugation mixtures were streaked onto a Sistrom's medium agar plate containing kanamycin (0.01 mg mL^{-1}) and succinate (10 mM). Plates were incubated in an Advanced™Anoxomat® III Anaerobic jar and placed 50 cm away from the light source in a light box chamber equipped with 8 incandescent white light bulbs (60 W, 120V, 840 lumens each). Single colonies were inoculated into 50 mL of Sistrom's medium supplemented with succinate (10 mM) and kanamycin (0.01 mg mL^{-1}) and grown photosynthetically in sealed bottles with N_2 gas in the headspace. For counter selection, cells were inoculated (10% v/v) into 500 mL of Sistrom's medium containing succinate (10 mM) and sucrose (0.3 M, added after autoclaving). After cultures reached full density (2–3 days), cells were harvested by

centrifugation at 6,000 x *g*. Pellets were re-suspended in 2–3 mL of Sistrom's medium, diluted in 10-fold increments, and a 0.1-mL sample was plated at dilutions 10^{-7} and 10^{-8}. Plates were incubated in an Advanced™Anoxomat® III Anaerobic jar and cells were grown photosynthetically as described above. Isolated colonies were screened using PCR for in-frame *bluE* deletions with primers listed in Table S3. Positive deletion strains were checked for kanamycin sensitivity to ensure loss of chromosomally inserted plasmid. For conjugations of complementation vector (pRsBluE10), the same protocol was followed up to incubation on Sistrom's agar plate with kanamycin.

Plasmid construction.

R. sphaeroides strain 2.4.1 and *R. capsulatus* strain SB1003 were gifts from Timothy Donohue (University of Wisconsin, Madison WI). Genomic DNA was isolated using Wizard® SV Genomic DNA Purification kit (Promega). Oligonucleotide primers were purchased from Integrated DNA Technologies Inc. Primers for cloning were designed using the Saccharomyces Genome Database web-based primer design tool http://www.yeastgenome.org/cgi-bin/web-primer. Genes were PCR amplified from the appropriate genomic DNA template with PCR Extender Polymerase (5 Prime) and the primer pairs listed in Table S3. PCR products and vectors were treated with FastDigest™ restriction endonucleases (Fermentas) indicated in the primer name in Table S3 and purified with the Wizard® SV Gel and PCR Clean-Up kit (Promega). Cloning vectors were treated with Fast AP alkaline phosphatase (Fermentas). PCR fragments and cloning vectors were ligated together using T4 Ligase (New England BioLabs) and introduced into *E. coli* DH5α (Raleigh *et al.*, 1989, Woodcock *et al.*, 1989) via electroporation (Calvin & Hanawalt, 1988). Plasmid DNA was purified using the Wizard® Plus SV Miniprep kit (Promega). Plasmid sequence was confirmed by sequencing using BigDye® (ABI PRISM) protocols, and sequencing reactions were resolved at the University of Wisconsin-Madison Biotechnology Center. The list of resulting plasmids can be found in Table S2. Primers for site directed mutagenesis were designed with the QuikChange Primer Design tool found at http://www.genomics.agilent.com/primerDesignProgram.jsp. DNA for site-directed mutagenesis was amplified using PfuUltra II Fusion DNA polymerase (Stratagene), and site-directed mutagenesis was performed using the QuikChange protocol from Stratagene. Genes used in this study were cloned into cloning vectors pBBR1MCS-2 (Kovach *et al.*, 1995) for complementation studies in *R. sphaeroides*, or pBAD24 and pBAD30 (Guzman *et al.*, 1995) for arabinose-dependent gene expression used in complementation studies in *S. enterica*. Plasmid pTEV5 (Rocco *et al.*, 2008) was used to overexpress the gene of interest to isolate protein needed for biochemical studies.

S. enterica growth media and conditions.

No-carbon essential (NCE) (Berkowitz *et al.*, 1968) was used as minimal growth medium with either glycerol (22 mM) or ethanolamine hydrochloride (90 mM) as the carbon and energy source. When added to the medium, the following supplements were at the indicated concentrations: trace minerals, (10 mL L^{-1}) (Balch & Wolfe, 1976); $MgSO_4$ (1 mM), 5,6-dimethylbenzimidazole (DMB, 0.15 mM), ampicillin (0.1 mg mL^{-1}), arabinose (0.5 mM). All corrinoids (dicyanocobyric acid [$(CN)_2$Cby], dicyanocobinamide [$(CN)_2$Cbi], and cyanocobalamin (CNCbl)) were added at 1 nM or 5 nM final concentration when glycerol

was used or 300 nM when ethanolamine was used as the carbon and energy source. Fe(III)-citrate (0.05 mM) was also added to the medium when ethanolamine was used. $(CN)_2$Cby was a gift from Paul Renz (Universität-Hohenheim, Stuttgart, Germany). When indicated L-Thr, L-Ser, L-Thr-P, and L-Ser were present in the medium at 1 mM. For growth analysis involving *Rs*BluE reactions, the reactions were filtered with sterile 0.2-μm Spin-X centrifuge filters (Corning) and added to the growth medium at 8% (v/v) concentration. All chemicals were purchased from Sigma-Aldrich. *S. enterica* strains were cultured in nutrient broth (NB, Difco Laboratories) (0.8% w/v) containing NaCl (85 mM). Lysogeny broth was used as rich medium to culture *E. coli* strains unless otherwise indicated. For complementation studies strains were grown in minimal medium in triplicate in sterile 96-well tissue culture plates (Falcon). A 1% (v/v) inoculum of an overnight cell culture grown in NB was used when glycerol was the carbon and energy source, and a 5% inoculum (v/v) was used for ethanolamine minimal medium in 0.2 mL total volume. Growth was monitored using Gen5 software (BioTek Instruments) at 37˚C with continuous shaking using the slow setting of an EL808 Ultra or PowerWave XS Microplate Reader (BioTek Instruments). Cell density measurements at 630 nm were acquired every 30 min for 24 or 72 h. Data were analyzed using the Prism v6 software package (GraphPad Software). Growth analyses were performed in triplicate in three independent experiments. Representative growth curves are shown with the error bars representing the standard error of the mean.

Rhodobacter growth medium, conditions, and analysis.

Relevant *R. sphaeroides* strains were grown for three days at 30°C in Sistrom's medium with succinate (10 mM) and kanamycin (0.01 mg mL^{-1}). Cells were washed twice with Sistrom's medium after centrifugation at 6,000 x *g* for 5 min. Cells were sub-cultured (1:50) into 0.2 mL Sistrom's medium with acetate (30 mM) and kanamycin and grown in a 96-well microtiter plate. Plates were incubated at 30°C inside a temperature-controlled chamber of a PowerWave XS Microplate Reader (BioTek Instruments). Plates were continuously shaken using the medium setting of the instrument and cell density was monitored at 630 nm. Data were analyzed using Prism v6 software package (GraphPad Software). Growth analyses were performed in triplicate in three independent experiments. Representative growth curves are shown with the error bars representing the standard error of the mean. Pigment analysis was performed with culture samples (100 μL) pipetted into a 96-well plate and scanned (A600–1000) using a Spectramax (Molecular Devices) UV-vis spectrophotometer.

Solubilization and enrichment of *Rs*BluE and *Se*PduX proteins.

E. coli C43 (λDE3) (JE6664) (Miroux & Walker, 1996) cells carrying plasmids pPDU23 or pRsBLUE4 encoding *N*-terminally His_6 tagged *S. enterica pduX*$^+$ or *R. sphaeroides bluE*$^+$ genes cloned into pTEV5 (Rocco *et al.*, 2008), respectively, were grown in 4 L of LB. *E. coli* does not encode PduX or homologues in its genome and is not known to synthesize or use L-Thr-P. Cells were centrifuged at 6,000 x *g* for 10 min. Cell pellets were placed at −20°C until used. Cell pellets were thawed in 30 mL of bind buffer [4-(2-hydroxyethyl)-1-piperazineethanesulfonic acid (HEPES-NaOH, 50 mM, pH 7.9 at 4°C), NaCl (500 mM), imidazole (5 mM)], and lysed (1.9×10^8 kPa) using a TS Series (1.1 kW) Bench top cell disrupter (Constant Systems Ltd.), equipped with a cooling jacket on the disruptor head to maintain a 6°C temperature using a Neslab ThermoFlex 900 recirculating chiller (Thermo

Scientific). Cell particulates were removed by centrifugation at 39,000 x *g* for 20 min. The supernatant containing soluble proteins was discarded. The pellet containing insoluble *Rs*BluE or *Se*PduX was re-suspended in 30 mL of bind buffer along with 12% (w/v) sarkosyl, followed by incubation at room temp for 30 min with shaking until the pellet was solubilized. Remaining debris was removed by centrifugation at 20,000 x *g* for 10 min. Sarkosyl was removed stepwise by dialysis into bind buffer containing 2% (w/v), then 1% (w/v) sarkosyl, followed by three rounds of dialysis into bind buffer without sarkosyl. Each dialysis step was performed in 2 L of buffer at 4ºC for 3 h. After the final dialysis the protein solution had approximately 1–2% sarkosyl present. The presence of solubilized protein was confirmed by SDS-PAGE (Laemmli, 1970) followed by staining with Coomassie Blue R (Sasse, 1991). Precipitated protein was removed by centrifugation at 20,000 x *g* for 10 min. Ni(NTA)-affinity chromatography was used with a 1.5-mL bed volume of HisPur Ni-NTA resin (Thermo Scientific). The column was equilibrated with bind buffer [HEPES (50 mM pH 7.9 at 4°C), NaCl (500 mM), imidazole (5 mM)] before supernatant was applied to the column. Due to the viscosity of the solution caused by sarkosyl, movement of the supernatant across the column was facilitated by using a P1 peristaltic pump (GE Healthcare) with a flow rate of 1 mL min^{-1}. After binding to the column, the column was washed with four column volumes of bind buffer, before proteins were eluted by stepwise increases in the imidazole concentration from 20 to 100 mM with 20-mM steps; 5-mL fractions were collected for each step. The His_6 tagged proteins did not bind to the column due to interference by sarkosyl and were found in the flow through. His_6 tagged proteins were treated with rTEV protease (1:100, rTEV:His_6-protein ratio) for 3 h at 25°C in bind buffer containing 1,4-dithiothreitol (DTT, 1 mM). It is unclear if the tag was removed, as sarkosyl-solubilized protein did not bind a Ni column. The protein was dialyzed into bind buffer containing ethylenediaminetetraacetic acid (EDTA, 1 mM) at room temperature for 1 h, then dialyzed twice more against the same buffer devoid of EDTA. Final dialysis was performed until the protein began to slowly precipitate to obtain the minimal concentration of sarkosyl required to maintain the enriched *Rs*BluE and *Se*PduX proteins in solution. Precipitated protein was removed by centrifugation at 6,000 x *g* for 5 min. Proteins were concentrated using Amicon Ultracel 10,000 MWCO centrifugal filters (Millipore), flash frozen drop-wise into liquid N_2, and stored at −80ºC until used. Further attempts to completely remove sarkosyl by treatment with BioBeads™ SM-2 Resin (BioRad) or Pierce™ Detergent Removal Spin (ThermoFisher) resulted in complete protein precipitation. Cells harboring the empty cloning vector, pTEV5, were subjected to the same purification process and sarkosyl solubilized extracts were used as a control for enzyme assays described below. Protein concentrations were determined using a NanoDrop 1000 spectrophotometer (Thermo Scientific), using the theoretical molecular weights and A_{280} molar extinction coefficients for each protein, which were obtained from the ExPASy Protparam database (Gasteiger *et al.*, 2003). Protein concentrations was verified using Bradford Assay Bio-Rad kit (Bradford, 1976). Proteins were resolved by SDS-PAGE. Protein purity was estimated using band densitometry with a Fotodyne imaging system and Foto/Analyst v.5.00 software (Fotodyne Inc.) for image acquisition and TotalLab v.2005 software for analysis (Nonlinear Dynamics). *Rs*BluE and *Se*PduX were purified to 70% purity.

Purification of detergent-free *Rs*BluE and *Se*PduX proteins.

Due to the partial potential effects of unfolding and concern of potential interference of sarkosyl on the enzymatic activity, we attempted to purify *Rs*BluE and *Se*PduX without sarkosyl or other detergents. Protein overexpression and cell lysis proceeded as described above with the exception that cell pellets were not frozen but used immediately after harvesting. Sarkosyl was not present in buffers, and after cell lysis and centrifugation to remove cellular debris, the soluble fraction was retained. The discarded insoluble fraction contained most of the overproduced proteins. The soluble fraction was applied to a HisPur Ni-NTA resin (Thermo Scientific) as described above. A small quantity of soluble His_6-tagged protein was bound to the resin and was eluted with imidazole (200 mM). This protein remained in solution for ~30–60 min before precipitating. Fractions containing soluble protein were immediately assayed for activity after elution from the column as described below. Figure S4 shows representative SDS-PAGE gels of whole cell extracts and fractions containing *Rs*BluE, *Se*PduX, and extracts from cells harboring the empty vector pTEV5, which was used as control. Protein purity was estimated using band densitometry with a Fotodyne imaging system and Foto/Analyst v.5.00 software (Fotodyne Inc.) for image acquisition and TotalLab v.2005 software for analysis (Nonlinear Dynamics). His_6-tagged *Rs*BluE and *Se*PduX were purified to 87% and 89% purity, respectively (Fig. 7A) Protein identity was verified by in-gel trypsin digestion, followed by MALDI mass spectrometry, peptide mass fingerprinting and protein identification via Mascot (Matrix Science) protein identification software and peptide sequence databases performed by the Proteomics and Mass Spectrometry Core Facility at the University of Georgia (Athens, GA). Previously published non-cleavable *C*- and *N*-terminally His tagged *Se*PduX proteins (Fan *et al.*, 2009, Fan & Bobik, 2008) were purified using published methods (Fan *et al.*, 2009) and those outlined above. Plasmids encoding non-cleavable *C*- and *N*-terminally His tagged *Se*PduX proteins were a gift from Thomas Bobik (Iowa State University).

ATPase activity assay.

ATPase activity was assessed using the ADP-Glo™ ATPase Assay kit (Promega) (Zegzouti *et al.*, 2009). Per the following manufacturer's instructions, this two-step endpoint assay was used in the following manner. Reaction mixtures containing ATP, L-Thr, and *Rs*BluE or *Se*PduX, were incubates for 1 hr and stopped with a proprietary reagent that depleted any remaining unused ATP. Then a secondary reagent was added, which converted the *Rs*BluE- or *Se*PduX-generated ADP back to ATP. ATP was then measured using an ATP-dependent luciferase reaction. The resulting luminescence was measured at 560 nm with a SpectraMax Plus Gemini EM microplate spectrophotometer (Molecular Devices) equipped with SoftMax Pro v4 software. Samples (25 μL each) taken from reaction mixtures containing HEPES buffer (50 mM, pH 7.9 at 25°C), $MgCl_2$ (1 mM), ATP (0.1 mM or 0.01 mM), L-Thr (0.01 mM or 10 mM), and sarkosyl-solubilized protein (0.14 μM or 12 μM) were incubated at 25°C for 1 h. A 5-μL sample of the reaction mixture was used in the ADP-Glo™ assay. Nunc 96-well round bottom black polypropylene microtiter plates (Thermo Fisher) were used to minimize background. ATP to ADP conversion was quantified from the luminescence (relative light units; RLU) after subtracting the background from the no-enzyme control and comparing the value to a standard curve of luminescence *vs* % ATP to ADP conversion (Fig. S3) and converted into units of ADP produced (mM) per mg of

protein. Reactions were performed in triplicate in two independent experiments. Error bars represent the standard deviation. For ATPase inhibition assays the following inhibitors were used adenosine diphosphate (ADP, 20 mM), sodium pyrophosphate (PPi, 10 mM), sodium phosphate monobasic (Pi, 10 mM), adenosine 5′-[γ-thio]triphosphate (ADP-γ-S, 0.2 mM), α,β-methyleneadenosine 5′-triphosphate (AMP-CPP, 10 mM), P1,P3-di(adenosine-5′) triphosphate ammonium salt (Ap3A, 10 mM).

Phosphorous nuclear magnetic resonance (^{31}P-NMR) analysis of the L-threonine kinase reaction products.

Proton-decoupled ^{31}P-NMR spectra were obtained using a Varian Unity Inova 500 MHz spectrometer (Chemical Sciences Magnetic Resonance Facility, University of Georgia, Athens, GA) with the following parameters: pulse angle 45°, relaxation delay 1 s, excitation pulse 3.88 μs, spectral width 12.11 kHz, acquisition time 0.81 s. Chemical shifts were referenced to a H_3PO_4 (85%) standard set to 0.0 ppm. Reaction mixtures (0.5 mL) consisted of HEPES buffer (50 mM, pH 7.5 at 25°C), $MgCl_2$ (1 mM), ATP (3 mM), L-Thr or L-Ser (6 mM). Immediately after elution from the Ni-NTA column, 10-μL samples of detergent-free protein (11 μM) were added to the reaction mixtures, which were incubated at 25°C for 1 h. Reaction mixtures used as negative controls contained L-Thr, L-Thr-P, L-Ser-P, Pi, and AMP (3 mM each), or ATP, sodium pyrophosphate (PPi), and sodium tripolyphosphate (PPPi) (6 mM each). Protein was removed from reaction mixtures by filtration using Amicon Ultracel filters (Millipore) with 10-kDa molecular mass size exclusion cut offs. Reaction mixtures were brought up to a final volume of 0.6 mL in D_2O (17% v/v). ^{31}P-NMR data were processed with MestReNova software version v7.0.0–8333 (Mestrelab Research). Representative spectra are shown from one of two independent reactions with detergent-free enzyme acquired from two independent protein purifications.

Spectrophotometric measurement of *Rs*BluE and *Se*PduX ATPase activities as a function of substrate.

ATPase activity were measured using an NADH-consuming assay (Bergmeyer *et al.*, 1985, Horswill & Escalante-Semerena, 2002, Wilson, 1962, Havemann & Bobik, 2003). All substrate stocks were made fresh. Reaction mixtures (0.1 mL) contained HEPES buffer (50 mM, pH 7.0 at 25°C), $MgCl_2$ (5 mM), phosphoenolpyruvate (PEP, 3 mM), NADH (0.1 mM), pyruvate kinase (1 U), lactate dehydrogenase (1.5 U); mixtures were incubated at 25°C with measurements taken every 11 s over a 20-min period. For the ATPase specific activity L-Thr concentration was held at 50 mM while the ATP concentration was varied (0–100 mM). To measure the effect of L-Thr on the ATPase activity, ATP concentration was held at 50 mM while the concentration of L-Thr was varied (0–100 mM). Reactions were started by the addition of *Rs*BluE or *Se*PduX (3 μM). The absorbance at 340 nm was monitored in a 96-well plate using the SpectraMax Plus UV-visible spectrophotometer (Molecular Devices) equipped with SoftMax Pro v6.2 software. Enzyme activities were calculated as described elsewhere (Wilson, 1962). Specific activity data are presented with standard deviations from two independent experiments performed in technical triplicate, with error bars representing the standard deviation.

Supplementary Material

Refer to Web version on PubMed Central for supplementary material.

Acknowledgments

The authors declare no conflict of interest. This work was supported by NIH grant R37 GM40313 to J.C.E.-S. N.K.T. was supported in part by NIH grant F31 GM095230 and Advanced Opportunity Fellowship awarded by the Graduate School of the University of Wisconsin, Madison. We thank Paul Renz (Universität Stuttgart) for his gift of $(CN)_2$Cby, Tim Donohue (University of Wisconsin-Madison) for providing *R. sphaeroides* strain 2.4.1 and *R. capsulatus* strain SB1003 (University of Wisconsin-Madison), and Paul Merchant for technical assistance. Thanks also to Dongtao Cui at the Chemical Sciences Magnetic Resonance facility (University of Georgia) for training and assistance with NMR experiments. We are grateful to Paula Pappalardo (University of Georgia) for assistance with R and phylogenetic analysis. Thank you to Thomas Bobik for providing plasmids encoding *pduX*.

References

Altschul SF, Madden TL, Schaffer AA, Zhang J, Miller W, and Lipmann DJ (1997) Gapped BLAST and PSI-BLAST: a new generation of protein database search programs. Nucl. Acids Res 25: 3389–3402. [PubMed: 9254694]

Amin SA, Green DH, Gardes A, Romano A, Trimble L, and Carrano CJ (2012) Siderophore-mediated iron uptake in two clades of *Marinobacter* spp. associated with phytoplankton: the role of light. Biometals 25: 181–192. [PubMed: 21947474]

Anderson PJ, Lango J, Carkeet C, Britten A, Kräutler B, Hammock BD, and Roth JR (2008) One pathway can incorporate either adenine or dimethylbenzimidazole as an alpha-axial ligand of B_{12} cofactors in *Salmonella enterica*. J. Bacteriol 190: 1160–1171. [PubMed: 17981976]

Andersson DI, and Roth JR (1989) Mutations affecting regulation of cobinamide biosynthesis in *Salmonella typhimurium*. J. Bacteriol 171: 6726–6733. [PubMed: 2687248]

Balch WE, and Wolfe RS (1976) New approach to the cultivation of methanogenic bacteria: 2-mercaptoethanesulfonic acid (HS-CoM)-dependent growth of *Methanobacterium ruminantium* in a pressurized atmosphere. Appl. Environ. Microbiol 32: 781–791. [PubMed: 827241]

Bandarian V, Pattridge KA, Lennon BW, Huddler DP, Matthews RG, and Ludwig ML (2002) Domain alternation switches B(12)-dependent methionine synthase to the activation conformation. Nat. Struct. Biol 9: 53–56. [PubMed: 11731805]

Banerjee R (2003) Radical carbon skeleton rearrangements: catalysis by coenzyme B12-dependent mutases. Chem. Rev 103: 2083–2094. [PubMed: 12797824]

Beck R, Raux E, Thermes C, Rambach A, and Warren M (1997) CbiX: a novel metal-binding protein involved in sirohaem biosynthesis in *Bacillus megaterium*. Biochem. Soc.Trans 25: 77S. [PubMed: 9056975]

Bergmeyer HU, Bergmeyer J, Grassl M, and Berger R (1985) Methods of enzymatic analysis. vol. iv "enzymes 2: Esterases, glycosidases, lyases, ligases". 3rd Edition Weinheim; Deerfield Beach, Florida; Basel: Verlag Chemie, 1984. 426 S., 258 DM. Acta Biotechnologica 5: 114–114.

Berkowitz D, Hushon JM, Whitfield HJ, Jr., Roth J, and Ames BN (1968) Procedure for identifying nonsense mutations. J. Bacteriol 96: 215–220. [PubMed: 4874308]

Bertani G (1951) Studies on lysogenesis. I. The mode of phage liberation by lysogenic *Escherichia coli*. J. Bacteriol 62: 293–300. [PubMed: 14888646]

Bertani G (2004) Lysogeny at mid-twentieth century: P1, P2, and other experimental systems. J. Bacteriol 186: 595–600. [PubMed: 14729683]

Biedendieck R, Malten M, Barg H, Bunk B, Martens JH, Deery E, Leech H, Warren MJ, and Jahn D (2010) Metabolic engineering of cobalamin (vitamin B12) production in *Bacillus megaterium*. Microb. Biotechnol 3: 24–37. [PubMed: 21255303]

Biel AJ (1992) Oxygen-regulated steps in Rhodobacter capsulatus tetrapyrrole biosynthetic pathway. J. Bacteriol 174: 5272–5274. [PubMed: 1644753]

Blanche F, Couder M, Debussche L, Thibaut D, Cameron B, and Crouzet J (1991) Biosynthesis of vitamin B12: stepwise amidation of carboxyl groups *b, d, e*, and *g* of cobyrinic acid *a,c*-diamide is

catalyzed by one enzyme in *Pseudomonas denitrificans*. J. Bacteriol 173: 6046–6051. [PubMed: 1917839]

Blanche F, Thibaut D, Debussche L, Hertle R, Zipfel F, and Muller G (1993) Parallels and decisive differences in vitamin-B12 biosyntheses. Angew. Chem. Int. Ed. Engl 32: 1651–1653.

Bork P, Sander C, and Valencia A (1993) Convergent evolution of similar enzymatic function on different protein folds: the hexokinase, ribokinase, and galactokinase families of sugar kinases. Protein Sci 2: 31–40. [PubMed: 8382990]

Bradbeer C, (1982) Cobalamin transport in microorganisms In: B12. Dolphin D (ed). New York: John Wiley & Sons, pp. 31–56.

Bradford MM (1976) A rapid and sensitive method for the quantitation of microgram quantities of protein utilizing the principle of protein-dye binding. Anal. Biochem 72: 248–254. [PubMed: 942051]

Buchan A, LeCleir GR, Gulvik CA, and Gonzalez JM (2014) Master recyclers: features and functions of bacteria associated with phytoplankton blooms. Nat. Rev. Microbiol 12: 686–698. [PubMed: 25134618]

Calvin NM, and Hanawalt PC (1988) High-efficiency transformation of bacterial cells by electroporation. J. Bacteriol 170: 2796–2801. [PubMed: 3286620]

Cameron B, Blanche F, Rouyez MC, Bisch D, Famechon A, Couder M, Cauchois L, Thibaut D, Debussche L, and Crouzet J (1991a) Genetic analysis, nucleotide sequence, and products of two Pseudomonas denitrificans cob genes encoding nicotinate-nucleotide: dimethylbenzimidazole phosphoribosyltransferase and cobalamin (5'-phosphate) synthase. J. Bacteriol 173: 6066–6073. [PubMed: 1917841]

Cameron B, Guilhot C, Blanche F, Cauchois L, Rouyez MC, Rigault S, Levy-Schil S, and Crouzet J (1991b) Genetic and sequence analyses of a *Pseudomonas denitrificans* DNA fragment containing two *cob* genes. J. Bacteriol 173: 6058–6065. [PubMed: 1917840]

Campbell GR, Taga ME, Mistry K, Lloret J, Anderson PJ, Roth JR, and Walker GC (2006) *Sinorhizobium meliloti bluB* is necessary for production of 5,6-dimethylbenzimidazole, the lower ligand of B12. Proc. Natl. Acad. Sci. U S A 103: 4634–4369. [PubMed: 16537439]

Collins HF, Biedendieck R, Leech HK, Gray M, Escalante-Semerena JC, McLean KJ, Munro AW, Rigby SE, Warren MJ, and Lawrence AD (2013) *Bacillus megaterium* has both a functional BluB protein required for DMB synthesis and a related flavoprotein that forms a stable radical species. PLoS One 8: e55708. [PubMed: 23457476]

Croft MT, Lawrence AD, Raux-Deery E, Warren MJ, and Smith AG (2005) Algae acquire vitamin B12 through a symbiotic relationship with bacteria. Nature 438: 90–93. [PubMed: 16267554]

Croft MT, Warren MJ, and Smith AG (2006) Algae need their vitamins. Eukaryot. Cell 5: 1175–1183. [PubMed: 16896203]

Crouzet J, Cameron B, Cauchois L, Rigault S, Rouyez MC, Blanche F, Thibaut D, and Debussche L (1990) Genetic and sequence analysis of an 8.7-kilobase *Pseudomonas denitrificans* fragment carrying eight genes involved in transformation of precorrin-2 to cobyrinic acid. J. Bacteriol 172: 5980–5990. [PubMed: 2211521]

Datsenko KA, and Wanner BL (2000) One-step inactivation of chromosomal genes in *Escherichia coli* K-12 using PCR products. Proc. Natl. Acad. Sci. USA 97: 6640–6645. [PubMed: 10829079]

Debussche L, Couder M, Thibaut D, Cameron B, Crouzet J, and Blanche F (1991) Purification and partial characterization of cob(I)alamin adenosyltransferase from *Pseudomonas denitrificans*. J. Bacteriol 173: 6300–6302. [PubMed: 1917862]

Doxey AC, Kurtz DA, Lynch MD, Sauder LA, and Neufeld JD (2015) Aquatic metagenomes implicate Thaumarchaeota in global cobalamin production. ISME J 9: 461–471. [PubMed: 25126756]

Drennan CL, Huang S, Drummond JT, Matthews RG, and Ludwig ML (1994) How a protein binds B_{12}: A 3.0Å X-ray structure of B_{12}-binding domains of methionine synthase. Science 266: 1669–1674. [PubMed: 7992050]

Edgar RC (2004) MUSCLE: multiple sequence alignment with high accuracy and high throughput. Nucleic Acids Res 32: 1792–1797. [PubMed: 15034147]

Erb TJ, Retey J, Fuchs G, and Alber BE (2008) Ethylmalonyl-CoA mutase from *Rhodobacter sphaeroides* defines a new subclade of coenzyme B12-dependent acyl-CoA mutases. J. Biol. Chem 283: 32283–32293. [PubMed: 18819910]

Escalante-Semerena JC (2007) Conversion of cobinamide into adenosylcobamide in bacteria and archaea. J. Bacteriol 189: 4555–4560. [PubMed: 17483216]

Escalante-Semerena JC, and Warren MJ, (2008) Biosynthesis and Use of Cobalamin (B_{12}) In: EcoSal - Escherichia coli and Salmonella: cellular and molecular biology. Böck A, Curtiss R, III, Kaper JB, Karp PD, Neidhardt FC, Nyström T, Slauch JM & Squires CL (eds). Washington, D. C.: ASM Press, pp.

Fan C, and Bobik TA (2008) The PDUX enzyme of *Salmonella enterica* is an L-threonine kinase used for coenzyme B_{12} synthesis. J. Biol. Chem 283: 11322–11329. [PubMed: 18308727]

Fan C, Fromm HJ, and Bobik TA (2009) Kinetic and functional analysis of L-threonine kinase, the PduX enzyme of *Salmonella enterica*. J. Biol. Chem 284: 20240–20248. [PubMed: 19509296]

FitzJohn RG (2012) Diversitree: comparative phylogenetic analyses of diversification in R. Meth. Ecol. Evol 3: 1084–1092.

Futagami T, Morono Y, Terada T, Kaksonen AH, and Inagaki F (2009) Dehalogenation Activities and Distribution of Reductive Dehalogenase Homologous Genes in Marine Subsurface Sediments. Appl. Environ. Microbiol 75: 6905–6909. [PubMed: 19749069]

Gasteiger E, Gattiker A, Hoogland C, Ivanyi I, Appel RD, and Bairoch A (2003) ExPASy: The proteomics server for in-depth protein knowledge and analysis. Nucleic Acids Res. 31: 3784–3788. [PubMed: 12824418]

Gonzalez JC, Banerjee RV, Huang S, Sumner JS, and Matthews RG (1992) Comparison of cobalamin-independent and cobalamin-dependent methionine synthases from *Escherichia coli*: two solutions to the same chemical problem. Biochemistry 31: 6045–6056. [PubMed: 1339288]

Gouet P, Courcelle E, Stuart DI, and Metoz F (1999) ESPript: multiple sequence alignments in PostScript. Bioinformatics 15: 305–308. [PubMed: 10320398]

Gough SP, Petersen BO, and Duus JO (2000) Anaerobic chlorophyll isocyclic ring formation in *Rhodobacter capsulatus* requires a cobalamin cofactor. Proc. Natl. Acad. Sci. U S A 97: 6908–6913. [PubMed: 10841582]

Gray MJ, and Escalante-Semerena JC (2007) Single-enzyme conversion of $FMNH_2$ to 5,6-dimethylbenzimidazole, the lower ligand of B_{12}. Proc. Natl. Acad. Sci. U S A 104: 2921–2926. [PubMed: 17301238]

Gray MJ, and Escalante-Semerena JC (2009a) The cobinamide amidohydrolase (cobyric acid-forming) CbiZ enzyme: a critical activity of the cobamide remodelling system of *Rhodobacter sphaeroides*. Mol. Microbiol 74: 1198–1210. [PubMed: 19889098]

Gray MJ, and Escalante-Semerena JC (2009b) In vivo analysis of cobinamide salvaging in *Rhodobacter sphaeroides* strain 2.4.1. J. Bacteriol 191: 3842–3851. [PubMed: 19376876]

Guindon S, Dufayard JF, Lefort V, Anisimova M, Hordijk W, and Gascuel O (2010) New algorithms and methods to estimate maximum-likelihood phylogenies: assessing the performance of PhyML 3.0. Syst. Biol 59: 307–321. [PubMed: 20525638]

Guzman LM, Belin D, Carson MJ, and Beckwith J (1995) Tight regulation, modulation, and high-level expression by vectors containing the arabinose PBAD promoter. J. Bacteriol 177: 4121–4130. [PubMed: 7608087]

Hall DA, Vander Kooi CW, Stasik CN, Stevens SY, Zuiderweg ER, and Matthews RG (2001) Mapping the interactions between flavodoxin and its physiological partners flavodoxin reductase and cobalamin-dependent methionine synthase. Proc. Natl. Acad. Sci. USA 98: 9521–9526. [PubMed: 11493691]

Harmon LJ, Weir JT, Brock CD, Glor RE, and Challenger W (2008) GEIGER: investigating evolutionary radiations. Bioinformatics 24: 129–131. [PubMed: 18006550]

Havemann GD, and Bobik TA (2003) Protein content of polyhedral organelles involved in coenzyme B12-dependent degradation of 1,2-propanediol in *Salmonella enterica* serovar Typhimurium LT2. J. Bacteriol 185: 5086–5095. [PubMed: 12923081]

Heal KR, Qin W, Ribalet F, Bertagnolli AD, Coyote-Maestas W, Hmelo LR, Moffett JW, Devol AH, Armbrust EV, Stahl DA, and Ingalls AE (2017) Two distinct pools of B12 analogs reveal

community interdependencies in the ocean. Proc. Natl. Acad. Sci. U S A 114: 364–369. [PubMed: 28028206]

Heldt D, Lawrence AD, Lindenmeyer M, Deery E, Heathcote P, Rigby SE, and Warren MJ (2005) Aerobic synthesis of vitamin B12: ring contraction and cobalt chelation. Biochem. Soc. Trans 33: 815–819. [PubMed: 16042605]

Hondorp ER, and Matthews RG (2004) Oxidative stress inactivates cobalamin-independent methionine synthase (MetE) in *Escherichia coli*. PLoS Biol 2: e336. [PubMed: 15502870]

Horswill AR, and Escalante-Semerena JC (2002) Characterization of the propionyl-CoA synthetase (PrpE) enzyme of *Salmonella enterica*: Residue Lys592 is required for propionyl-AMP synthesis. Biochemistry 41: 2379–2387. [PubMed: 11841231]

Jakubowski H (1990) Proofreading in vivo: editing of homocysteine by methionyl-tRNA synthetase in Escherichia coli. Proc. Natl. Acad. Sci 87: 4504–4508. [PubMed: 2191291]

Jones DT, Taylor WR, and Thornton JM (1992) The Rapid Generation of Mutation Data Matrices From Protein Sequences. Comput. Appl. Biosci 8: 275–282. [PubMed: 1633570]

Keller S, Kunze C, Bommer M, Paetz C, Menezes RC, Svatos A, Dobbek H, and Schubert T (2018) Selective Utilization of Benzimidazolyl-Norcobamides as Cofactors by the Tetrachloroethene Reductive Dehalogenase of Sulfurospirillum multivorans. J Bacteriol 200.

Keller S, Ruetz M, Kunze C, Krautler B, Diekert G, and Schubert T (2013) Exogenous 5,6-dimethylbenzimidazole caused production of a non-functional tetrachloroethene reductive dehalogenase in *Sulfurospirillum multivorans*. Environ. Microbiol 16: 3361–3369. [PubMed: 24433392]

Keller S, Ruetz M, Kunze C, Krautler B, Diekert G, and Schubert T (2014) Exogenous 5,6-dimethylbenzimidazole caused production of a non-functional tetrachloroethene reductive dehalogenase in Sulfurospirillum multivorans. Environ. Microbiol 16: 3361–3369. [PubMed: 24433392]

Keller S, Treder A, von Reuss SH, Escalante-Semerena JC, and Schubert T (2016) The SMUL_1544 Gene Product Governs Norcobamide Biosynthesis in the Tetrachloroethene-Respiring Bacterium Sulfurospirillum multivorans. J Bacteriol 198: 2236–2243. [PubMed: 27274028]

Kovach ME, Elzer PH, Hill DS, Robertson GT, Farris MA, Roop RM, 2nd, and Peterson KM (1995) Four new derivatives of the broad-host-range cloning vector pBBR1MCS, carrying different antibiotic-resistance cassettes. Gene 166: 175–176. [PubMed: 8529885]

Kräutler B, Fieber W, Osterman S, Fasching M, Ongania K-H, Gruber K, Kratky C, Mikl C, Siebert A, and Diekert G (2003) The cofactor of tetrachloroethene reductive dehalogenase of *Dehalospirillum multivorans* is Norpseudo-B12, a new type of natural corrinoid. Helv. Chim. Acta 86: 3698–3716.

Laemmli UK (1970) Cleavage of structural proteins during the assembly of the head of bacteriophage T4. Nature 227: 680–685. [PubMed: 5432063]

Leech HK, Raux-Deery E, Heathcote P, and Warren MJ (2002) Production of cobalamin and sirohaem in Bacillus megaterium: an investigation into the role of the branchpoint chelatases sirohydrochlorin ferrochelatase (SirB) and sirohydrochlorin cobalt chelatase (CbiX). Biochem. Soc. Trans 30: 610–613. [PubMed: 12196147]

Liu J, Lopez N, Ahn Y, Goldberg T, Bromberg Y, Kerkhof LJ, and Haggblom MM (2017) Novel Reductive Dehalogenases From The Marine Sponge Associated Bacterium Desulfoluna spongiiphila. Environ. Microbiol. Rep 9: 537–549. [PubMed: 28618195]

Markowitz VM, Korzeniewski F, Palaniappan K, Szeto E, Werner G, Padki A, Zhao X, Dubchak I, Hugenholtz P, Anderson I, Lykidis A, Mavromatis K, Ivanova N, and Kyrpides NC (2006) The integrated microbial genomes (IMG) system. Nucleic Acids Res 34: D344–348. [PubMed: 16381883]

Mattes TA, Deery E, Warren MJ, and Escalante-Semerena JC, (2017) Cobalamin Biosynthesis and Insertion In: Encyclopedia of Inorganic and Bioinorganic Chemistry. Scott RA (ed). Chichester, UK: John Wiley & Sons, Ltd, pp. 1–24.

McGoldrick HM, Roessner CA, Raux E, Lawrence AD, McLean KJ, Munro AW, Santabarbara S, Rigby SE, Heathcote P, Scott AI, and Warren MJ (2005) Identification and characterization of a novel vitamin B12 (cobalamin) biosynthetic enzyme (CobZ) from *Rhodobacter capsulatus*, containing flavin, heme, and Fe-S cofactors. J. Biol. Chem 280: 1086–1094. [PubMed: 15525640]

Miroux B, and Walker JE (1996) Over-production of proteins in *Escherichia coli*: mutant hosts that allow synthesis of some membrane proteins and globular proteins at high levels. J. Mol. Biol 260: 289–298. [PubMed: 8757792]

Moore SJ, Lawrence AD, Biedendieck R, Deery E, Frank S, Howard MJ, Rigby SE, and Warren MJ (2013) Elucidation of the anaerobic pathway for the corrin component of cobalamin (vitamin B12). Proc. Natl. Acad. Sci. U S A 110: 14906–14911. [PubMed: 23922391]

O'Toole GA, Rondon MR, and Escalante-Semerena JC (1993) Analysis of mutants of defective in the synthesis of the nucleotide loop of cobalamin. J. Bacteriol 175: 3317–3326. [PubMed: 8501035]

Paradis E, Claude J, and Strimmer K (2004) APE: Analyses of phylogenetics and evolution in R language. Bioinformatics 20: 289–290. [PubMed: 14734327]

Peariso K, Zhou ZS, Smith AE, Matthews RG, and Penner-Hahn JE (2001) Characterization of the zinc sites in cobalamin-independent and cobalamin-dependent methionine synthase using zinc and selenium X-ray absorption spectroscopy. Biochemistry 40: 987–993. [PubMed: 11170420]

Pollich M, and Klug G (1995) Identification and sequence analysis of genes involved in late steps of cobalamin (vitamin B12) synthesis in *Rhodobacter capsulatus*. J. Bacteriol 177: 4481–4487. [PubMed: 7635831]

Pollich M, Wersig C, and Klug G (1996) The *bluF* gene of *Rhodobacter capsulatus* is involved in conversion of cobinamide to cobalamin (vitamin B_{12}). J. Bacteriol 178: 7308–7310. [PubMed: 8955417]

R Core Development Team, (2015) R: A language and environment for statistical computing. In. Vienna, Austria: R Foundation for Statistical Computing, pp.

Raleigh EA, Lech K, and Brent R, (1989) Selected topics from classical bacterial genetics In: Curr. Protoc. Mol. Biol Ausubel FA, Brent R, Kingston RE, Moore DD, Seidman JG, Smith JA & Struhl K (eds). New York: Wiley Interscience, pp. 1.4.

Rambaut A, (2007) FigTree In. University of Edinburgh, Edinburgh UK: Institute of Evolutionary Biology, University of Edinburgh, Ashworth Laboratories pp. FigTree is designed as a graphical viewer of phylogenetic trees and as a program for producing publication-ready figures..

Raux E, Lanois A, Levillayer F, Warren MJ, Brody E, Rambach A, and Thermes C (1996) *Salmonella typhimurium* cobalamin (vitamin B_{12}) biosynthetic genes: functional studies in *S. typhimurium* and *Escherichia coli*. J. Bacteriol 178: 753–t767. [PubMed: 8550510]

Raux E, Lanois A, Warren MJ, Rambach A, and Thermes C (1998) Cobalamin (vitamin B_{12}) biosynthesis: identification and characterization of a *Bacillus megaterium cobI* operon. Biochem. J 335: 159–166. [PubMed: 9742225]

Rocco CJ, Dennison KL, Klenchin VA, Rayment I, and Escalante-Semerena JC (2008) Construction and use of new cloning vectors for the rapid isolation of recombinant proteins from *Escherichia coli*. Plasmid 59: 231–237. [PubMed: 18295882]

Rodionov DA, Vitreschak AG, Mironov AA, and Gelfand MS (2003) Comparative genomics of the vitamin B_{12} metabolism and regulation in prokaryotes. J. Biol. Chem 278: 41148–41159. [PubMed: 12869542]

Roessner CA, Santander PJ, and Scott AI (2001) Multiple biosynthetic pathways for vitamin B12: variations on a central theme. Vitam. Horm 61: 267–297. [PubMed: 11153269]

Roof DM, and Roth JR (1988) Ethanolamine utilization in *Salmonella typhimurium*. J. Bacteriol 170: 3855–3863. [PubMed: 3045078]

Roof DM, and Roth JR (1989) Functions required for vitamin B12-dependent ethanolamine utilization in *Salmonella typhimurium*. J. Bacteriol 171: 3316–3323. [PubMed: 2656649]

Sasse J, (1991) Detection of proteins In: Curr. Protoc. Mol. Biol Ausubel FA, Brent R, Kingston RE, Moore DD, Seidman JG, Smith JA & Struhl K (eds). New York: Wiley Interscience, pp. 10.16.11–10.16.18.

Schroeder S, Lawrence AD, Biedendieck R, Rose RS, Deery E, Graham RM, McLean KJ, Munro AW, Rigby SE, and Warren MJ (2009) Demonstration that CobG, the monooxygenase associated with the ring contraction process of the aerobic cobalamin (vitamin B12) biosynthetic pathway, contains a Fe-S center and a mononuclear non-heme iron center. J. Biol. Chem 284: 4796–4805. [PubMed: 19068481]

Sistrom WR (1960) A requirement for sodium in the growth of *Rhodopseudomonas spheroides*. J. Gen. Microbiol 22: 778–785. [PubMed: 14447230]

Smith DM, Fraga H, Reis C, Kafri G, and Goldberg AL (2011) ATP binds to proteasomal ATPases in pairs with distinct functional effects, implying an ordered reaction cycle. Cell 144: 526–538. [PubMed: 21335235]

Taga ME, Larsen NA, Howard-Jones AR, Walsh CT, and Walker GC (2007) BluB cannibalizes flavin to form the lower ligand of vitamin B12. Nature 446: 449–453. [PubMed: 17377583]

Tavares NK, Zayas CL, and Escalante-Semerena JC (2018) The *Methanosarcina mazei* MM2060 gene encodes a bifunctional kinase/decarboxylase enzyme involved in cobamide biosynthesis. Biochemistry, doi: 10.1021/acs.biochem.8b00546; published online on 6.27/2018

Taylor RT, and Weissbach H, (1973) N^5-methylenetetrahydrofolate-homocysteine methyltransferases In: The Enzymes. Boyer PD (ed). New York: Academic Press, Inc., pp. 121–165.

Thibaut D, Couder M, Crouzet J, Debussche L, Cameron B, and Blanche F (1990) Assay and purification of S-adenosyl-L-methionine:precorrin-2 methyltransferase from *Pseudomonas denitrificans*. J. Bacteriol 172: 6245–6251. [PubMed: 2172210]

Vlcek C, Paces V, Maltsev N, Paces J, Haselkorn R, and Fonstein M (1997) Sequence of a 189-kb segment of the chromosome of Rhodobacter capsulatus SB1003. Proc. Natl. Acad. Sci. U. S. A 94: 9384–9388. [PubMed: 9256491]

Willows RD, and Kriegel AM, (2009) Biosynthesis of bacteriochlorophylls in purple bacteria. In: The Purple Phototrophic Bacteria, Advances in Photosynthesis and Respiration Hunter N, Daldal F, Thurnauer MC & Beatty JT (eds). Berlin: Springer Science+Business Media BV, pp. 57–79.

Wilson AC P. a.A.B. (1962) Regulation of flavin synthesis by *Escherichia coli*. J. Gen. Microbiol 28: 283–303. [PubMed: 14007303]

Woodcock DM, Crowther PJ, Doherty J, Jefferson S, De Cruz E, Noyer-Weidner M, Smith SS, Michael MZ, and Graham MW (1989) Quantitative evaluation of *Escherichia coli* host strains for tolerance to cytosine methylation in plasmid and phage recombinants. Nucl. Acids Res 17: 3469–3478. [PubMed: 2657660]

Woodson JD, and Escalante-Semerena JC (2004) CbiZ, an amidohydrolase enzyme required for salvaging the coenzyme B_{12} precursor cobinamide in archaea. Proc. Natl. Acad. Sci. USA 101: 3591–3596. [PubMed: 14990804]

Woodson JD, Zayas CL, and Escalante-Semerena JC (2003) A new pathway for salvaging the coenzyme B_{12} precursor cobinamide in archaea requires cobinamide-phosphate synthase (CbiB) enzyme activity. J. Bacteriol 185: 7193–7201. [PubMed: 14645280]

Yin L, and Bauer CE (2013) Controlling the delicate balance of tetrapyrrole biosynthesis. Philos. Trans. R. Soc. Lond. B. Biol. Sci 368: 20120262. [PubMed: 23754814]

Zayas CL, Claas K, and Escalante-Semerena JC (2007) The CbiB protein of *Salmonella enterica* is an integral membrane protein involved in the last step of the de novo corrin ring biosynthetic pathway. J. Bacteriol 189: 7697–7708. [PubMed: 17827296]

Zayas CL, and Escalante-Semerena JC (2007) Reassessment of the late steps of coenzyme B_{12} synthesis in *Salmonella enterica*: Evidence that dephosphorylation of adenosylcobalamin-5'-phosphate by the CobC phosphatase is the last step of the pathway. J. Bacteriol 189: 2210–2218. [PubMed: 17209023]

Zegzouti H, Zdanovskaia M, Hsiao K, and Goueli SA (2009) ADP-Glo: A Bioluminescent and homogeneous ADP monitoring assay for kinases. Assay Drug Dev. Technol 7: 560–572. [PubMed: 20105026]

Zumft WG (1997) Cell biology and molecular basis of denitrification. Microbiol. Mol. Biol. Rev 61: 533–616. [PubMed: 9409151]

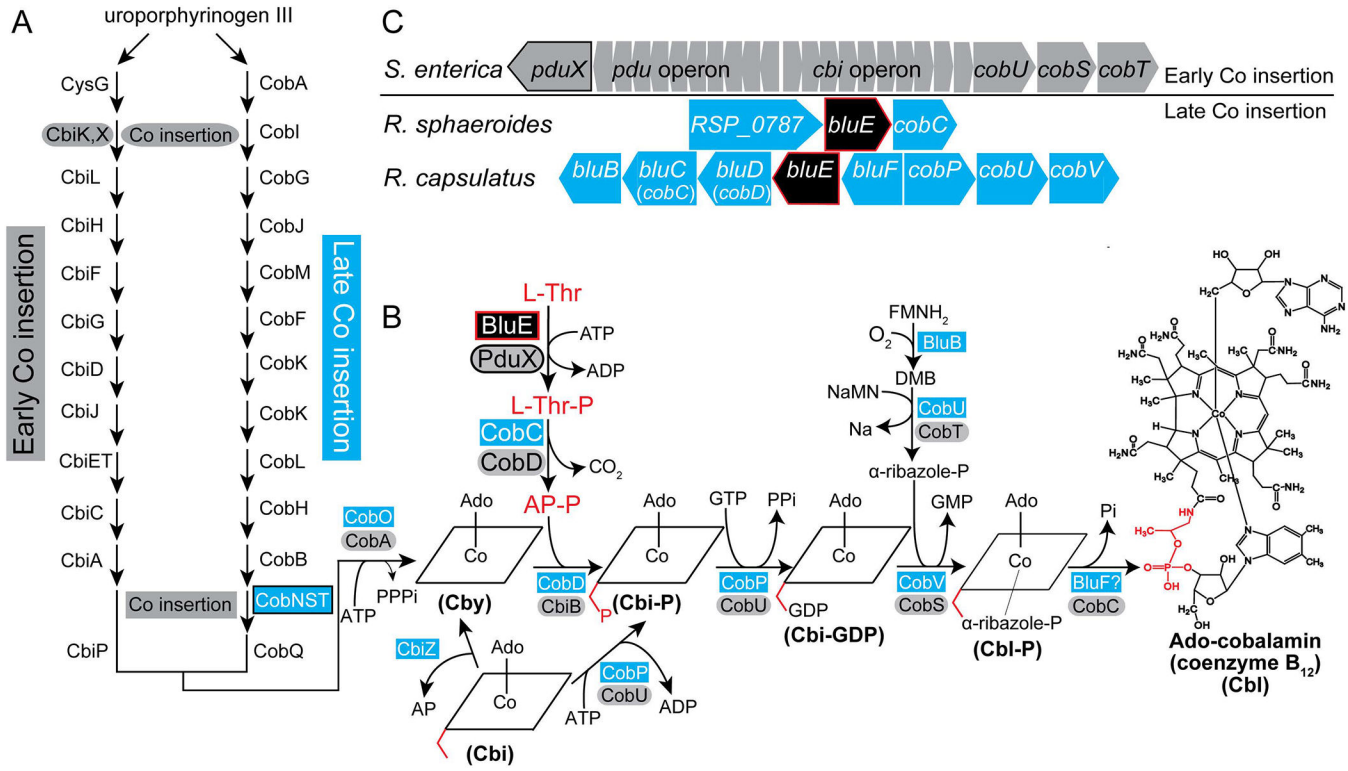

Figure 1. AdoCbl biosynthetic pathways in bacteria and archaea.

A. Schematic depicting the early- and late-cobalt insertion pathways of AdoCbl biosynthesis. B. Late steps of the AdoCbl biosynthetic pathway, with proteins in the early-cobalt-insertion (a.k.a. O_2-independent, blue rectangles) and late-cobalt-insertion (a.k.a. O_2-dependent, gray ovals) pathways. The BluE enzyme is shown in a black box with red trim. The (*R*)-1-aminopropan-2-ol *O*-phosphate (AP-P) moiety is highlighted in red in the structure scheme. Exogenous Cbi (a.k.a $(CN)_2$Cbi) enters the pathway as indicated. Exogenous Cby (a.k.a $(CN)_2$Cby) enters the pathway at the location it appears on in the figure. Exogenous corrinoids, including complete Cbas such as Cbl are adenylated by CobA/CobO upon transport into the cell and prior to entering the pathway. C. Genetic layout of the L-threonine kinase-encoding genes *bluE* in the late-cobalt-insertion, AdoCbl-synthesizing bacteria *R. sphaeroides* and *R. capsulatus*, and *pduX* in *S. enterica*, an early-cobalt-insertion, AdoCbl-synthesizing bacterium. Figure key: Ado, Adenosyl; Cby, cobyric acid; Cbi-P, cobinamide phosphate; Cbi-GDP, cobinamide-GDP; Cbl-P, cobalamin phosphate; Cbl, cobalamin; AP-P, (*R*)-1-aminopropan-2-ol *O*-phosphate; AP, (*R*)-1-aminopropan-2-ol; L-Thr-P, L-threonine-*O*-3-phosphate; L-Thr, L-threonine; α-ribazole-P, α-ribazole phosphate; DMB, 5,6-dimethylbenzimidazole; NaMN, nicotinic acid mononucleotide; Nm, Nicotinic Acid; PPi, pyrophosphate; Pi, orthophosphate; CbiK/CbiX, anaerobic cobaltochelatase; CobN/CobS/CobT, aerobic hydrogenobyrinic acid *a,c*-diamide cobaltochelatase; CobA/CobO, ATP:Co(I)rrinoid Adenosyltransferase; CbiB/CobD, AdoCbi-P synthase; CobS/CobV, AdoCba-5′P synthase; CobD/CobC, L-Thr-P decarboxylase; CobT/CobU, NaMN:DMB phosphoribosyltransferase; CobU/CobP, AdoCbi kinase / AdoCbi-P guanylyltransferase; PduX/BluE, L-Thr kinase; CobC/BluF, AdoCba-5′-P phosphatase; CbiZ, cobinamide amidohydrolase; *pdu*, genes of the Cba-dependent 1,2-propanediol

degradation operon; *cbi*, genes of the early steps of the early-Co-insertion cobalamin biosynthesis operon.

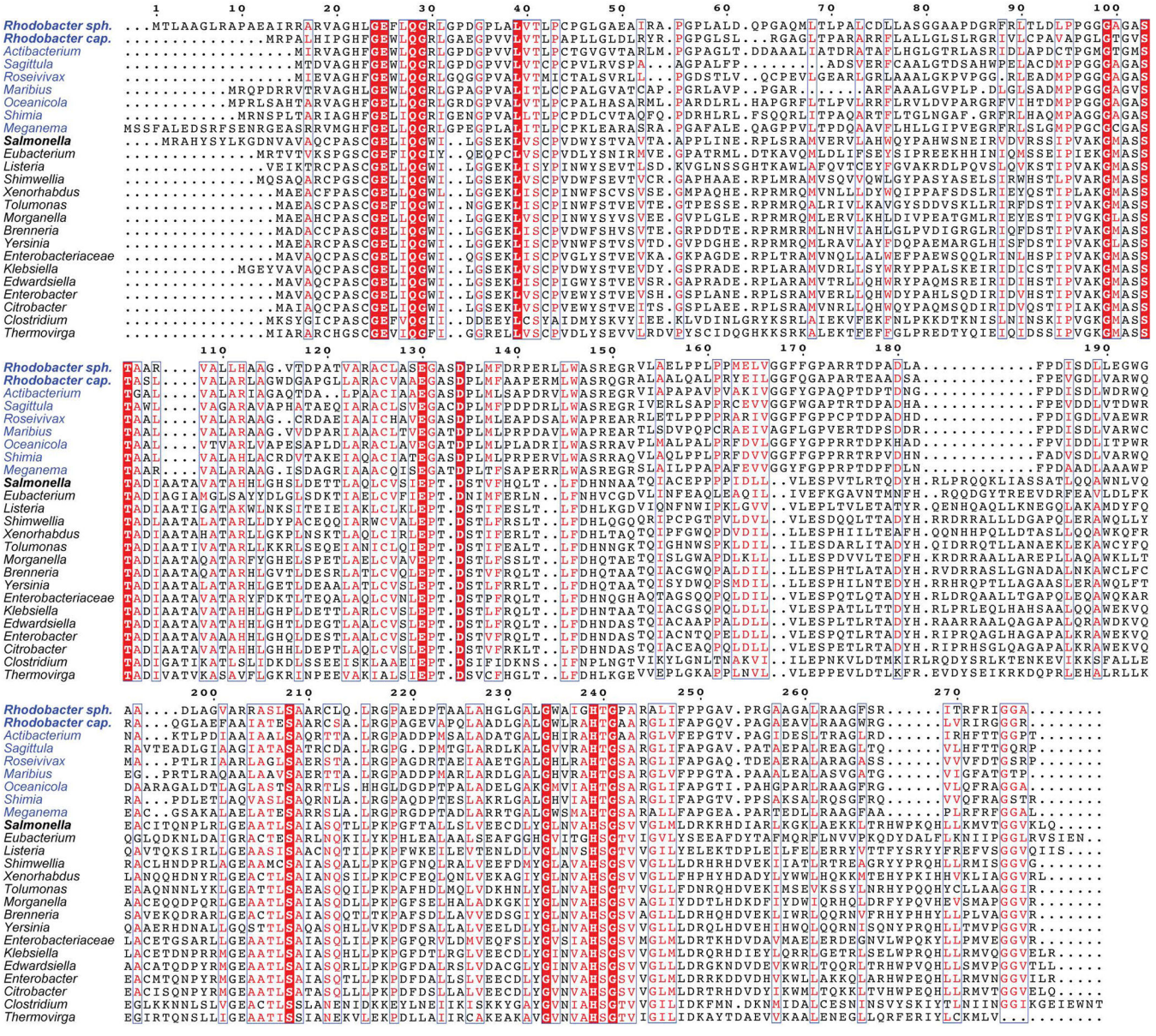

Figure 2. Sequence alignment of representative PduX and BluE proteins.

Genera names of organisms with BluE homologues are colored blue and PduX homologues are colored black. Residues that are 100% conserved are highlighted in red with white lettering. Areas with a high degree of conservation greater than 75% but less than 100% and or residues with similar properties are boxed in blue with red letter.

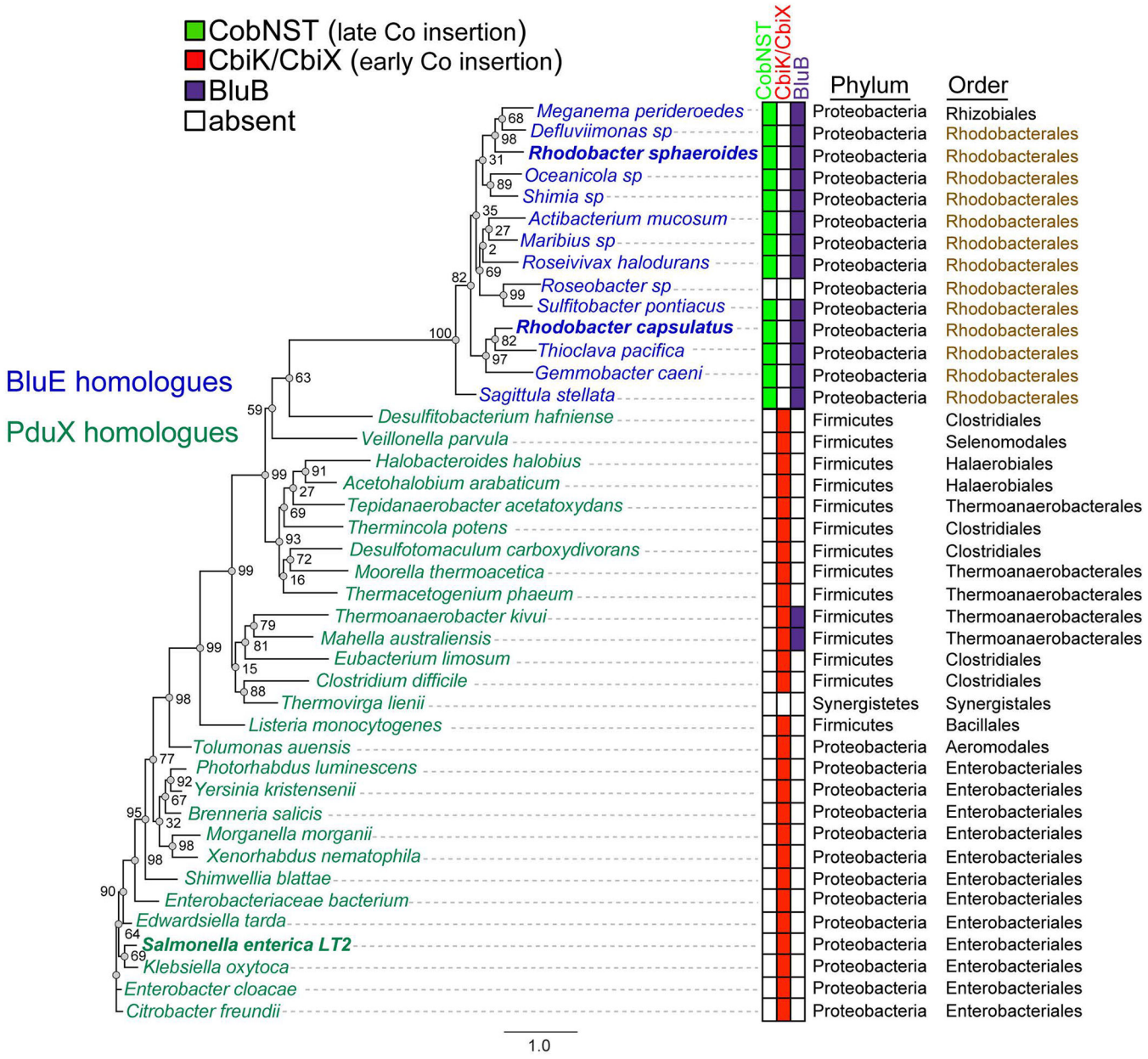

Figure 3. Phylogenetic analysis of the distribution of PduX and BluE proteins.

Maximum likelihood phylogenetic tree of homologous proteins based on the amino acid sequence of *Se*PduX (dark green) and *Rs*BluE or *Rc*BluE (blue). Order *Rhodobacterales* is highlighted in brown. Color-coded table of the presence or absence of the cobaltochelatase CbiK or CbiX (red squares), which is indicative of the early-cobalt-insertion pathway, the presence of all three subunits of the cobaltochelatase CobNST (lime green squares) in organisms that use the late-cobalt-insertion pathway and BluB (purple squares) the O_2-dependent DMB synthase, which is indicative of a physiological reliance on Cbas with DMB as the lower ligand base. Sequences were aligned using the MUSCLE (Edgar, 2004) plugin within Geneious R8.1.7 software (Biomatters Ltd.) with 100 iterations and default settings. Maximum likelihood phylogenic tree was generated with the online PhyML

(Guindon *et al.*, 2010) tool on the ATCG Montpellier Bioinformatics Platform available at http://www.atgc-montpellier.fr/phyml/, using Jones-Taylor-Thornton substitution model (Jones *et al.*, 1992) with 500 bootstrap replicates. Bootstrap support for each node is shown as a percent value. The scale bar is provided as a reference for branch lengths. Gene locus tags are available in Table S1.

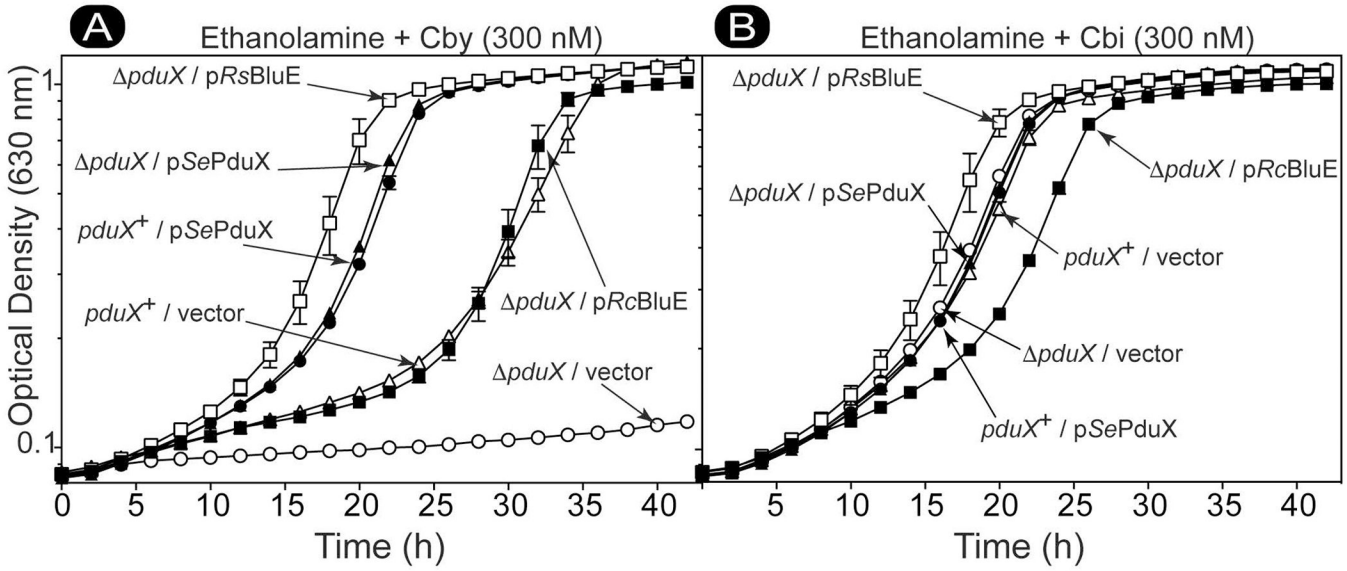

Figure 4. *Rs*BluE and *Rc*BluE restore AdoCbl synthesis in a *S. enterica* Δ*pduX* strain.

Growth analysis of *S. enterica pduX*$^+$ and Δ*pduX* strains harboring plasmids expressing *bluE*$^+$ from *R. sphaeroides* (*R.s. bluE*$^+$), *R. capsulatus* (*R.c. bluE*$^+$), PduX from *S. enterica* (*S.e. pduX*$^+$), or containing the empty vector pBAD24 (vector). Cells grown aerobically at 37°C in NCE minimal medium with ethanolamine (90 mM) as the sole carbon and energy source, supplemented with DMB (0.15 mM), arabinose (0.5 mM), ampicillin (0.1 mg mL^{-1}), $MgSO_4$ (1 mM), Fe(III)-citrate (0.05 mM), and A. Cby (300 nM) or B. Cbi (300 nM). A representative graph of three independent growth experiments performed in technical triplicate. Error bar represent the standard error of the mean. Figure key: Δ*pduX*/p*Rs*BluE (□), Δ*pduX*/p*Se*PduX (▲), Δ*pduX*/p*Rc*BluE (■), Δ*pduX*/vector (○), *pduX*$^+$/p*Se*PduX (●), *pduX*$^+$/vector (△).

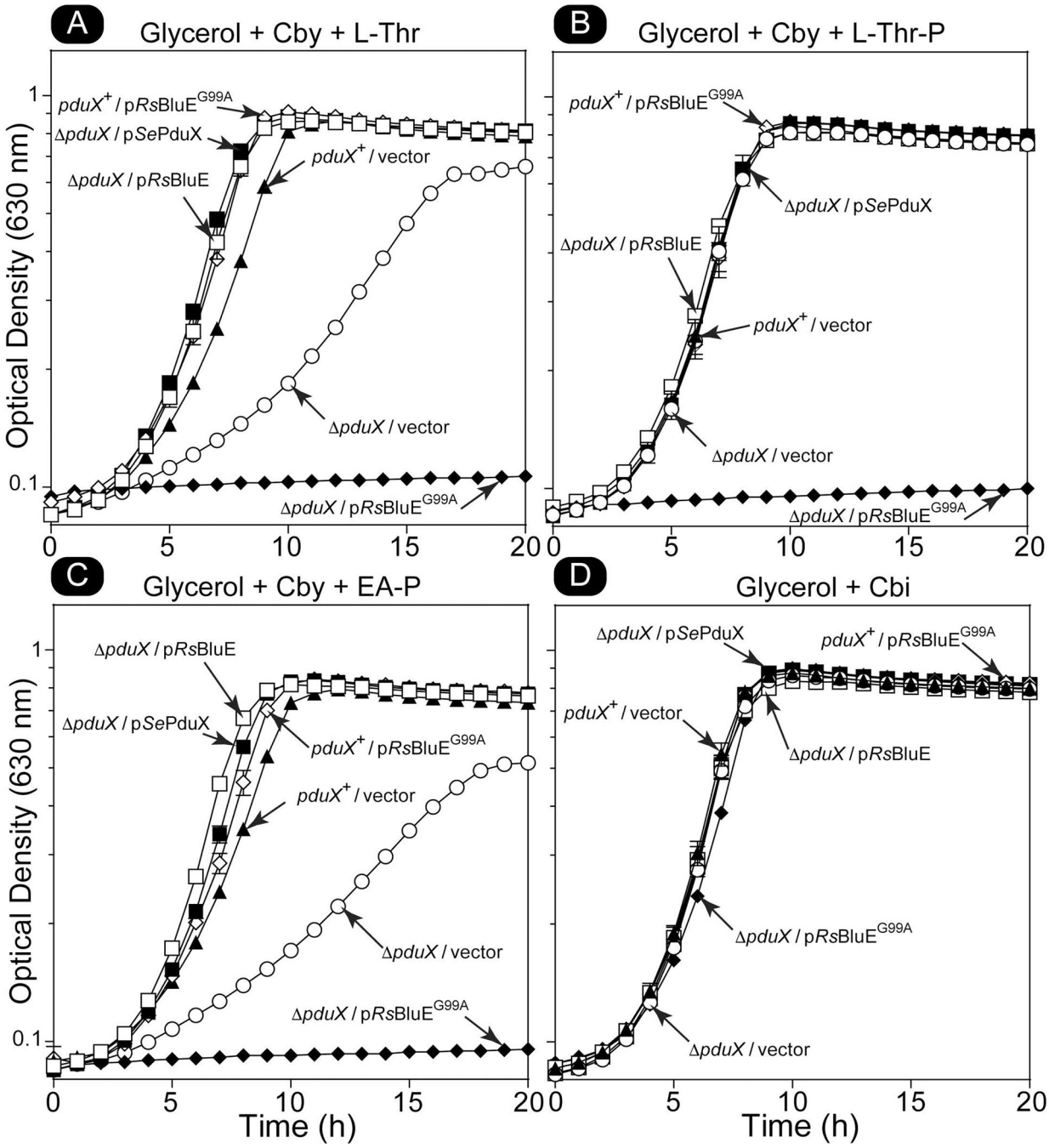

Figure 5. *Rs*BluE^{G99A} variant disrupts all the enzymes in the entire AP-P synthesis and attachment branch in *S. enterica in vivo*.

Representative graphs of growth analyses of *S. enterica* cells grown aerobically at 37°C in NCE minimal medium with glycerol (22 mM) ampicillin (0.1 mg mL^{-1}), and $MgSO_4$ (1 mM) Cby (1 nM) and supplemented with A. L-Thr (1 mM), B. L-Thr-P (1 mM), or C. ethanolamine phosphate (EA-P, 1 mM). Cbi (1 mM) was used as the corrinoid in place of Cby in panel D. Experiments were replicated in two independent experiments, each performed in triplicate. Error bar represent the standard error of the mean. Figure key:

Δ*pduX*/p*Rs*BluE (□), Δ*pduX*/p*Se*PduX (■), Δ*pduX*/p*Rs*BluE^{G99A} (◆), *pduX*$^{+}$/p*Rs*BluE^{G99A} (◇), *pduX*$^{+}$/vector (▲), Δ*pduX*/vector (○).

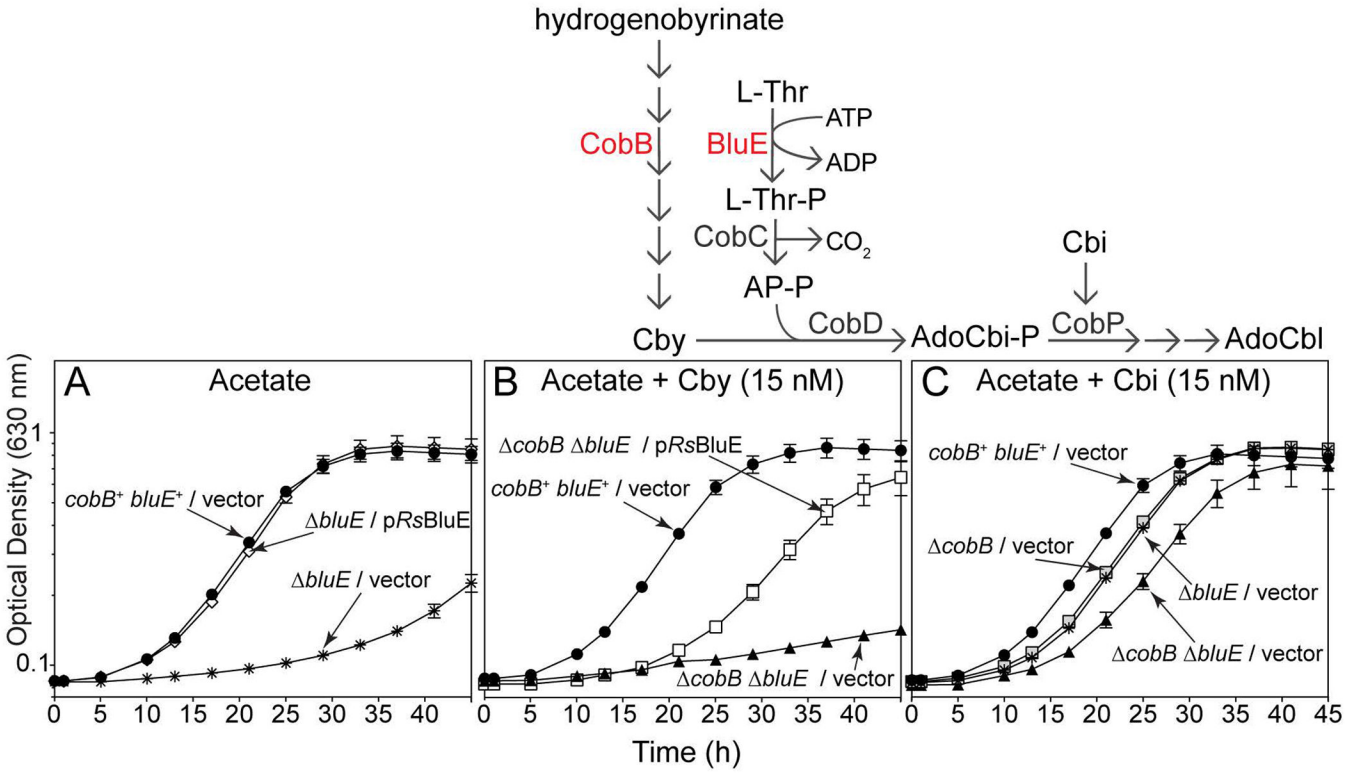

Figure 6. Growth analysis of *R. sphaeroides* Δ*bluE* and Δ*bluE* Δ*cobB* strains.

Growth analysis of *R. sphaeroides bluE*$^+$, Δ*bluE*, and Δ*cobB* Δ*bluE* strains harboring a plasmid expressing *R. sphaeroides bluE*$^+$ or carrying the empty pBBR1MCS-2 plasmid (vector). Cells were grown overnight in Sistrom's medium and cultures were prepared as described in *Materials and Methods*. Cell growth was monitored normoxically at 30°C in Sistrom's medium with acetate (30 mM), kanamycin (0.01 mg mL^{-1}), and when noted, Cby (15 nM) or Cbi (15 nM). Growth experiments were performed in triplicate in three independent experiments. Error bars represent the standard error of the mean. Pathway represents a simplified schematic of the roles of CobB (hydrogenobyrinate *a,c*-diamide synthase) and BluE (L-Thr kinase) in the synthesis of cobalamin in *R. sphaeroides*. CobD, AdoCbi-P synthase; CobC, L-Thr-P decarboxylase; CobP, AdoCbi kinase / AdoCbi-P guanylyltransferase; BluE, L-Thr kinase; Cby, cobyric acid; Cbi, cobinamide, AP-P, (*R*)-1-aminopropan-2-ol *O*-phosphate. Figure key: Panel A: *cobB*$^+$ *bluE*$^+$/vector (●), Δ*bluE*/p*Rs*BluE (○), Δ*bluE*/vector (✳), Panel B: Δ*cobB* Δ*bluE*/p*Rs*BluE (□), Δ*cobB* Δ*bluE*/vector (▲), *cobB*$^+$ *bluE*$^+$/p*Rs*BluE (●), Panel C: *cobB*$^+$ *bluE*$^+$/vector (●), Δ*cobB* Δ*bluE*/vector (▲), Δ*cobB*/vector (□), Δ*bluE*/vector (✳).

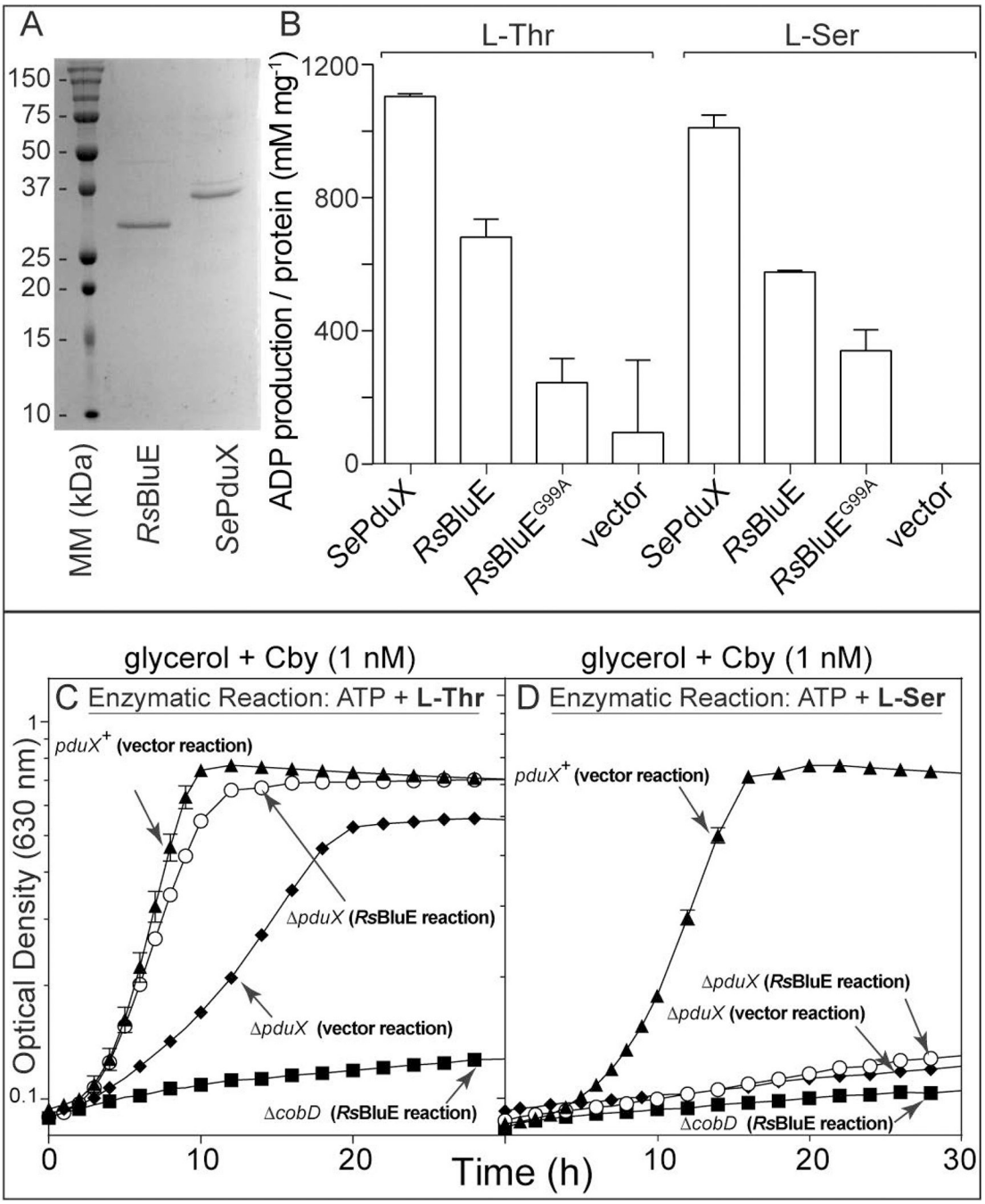

Figure 7. ***In vitro*** **ATPase activity assay for** ***Rs*****BluE.**

A. SDS-PAGE-gel of purified, sarkosyl-solubilized *Rs*BluE and *Se*PduX. B. ATPase activity assay performed with ADP-Glo™ ATPase Assay kit (Promega). Reaction mixtures contained HEPES buffer (50 mM, pH 7.0 at 25°C), $MgCl_2$ (1 mM), ATP (0.1 mM), L-Thr or L-Ser (10 mM), enrichment samples of *Se*PduX, *Rs*BluE, and *Rs*BluE^{G99A} sarkosyl-solubilized protein (12 μM) incubated at 25°C for 1 h. Negative control reaction mixtures contained extracts of sarkosyl-solubilized protein obtained from cells expressing the empty overexpression vector pTEV5 (vector). ATP to ADP conversion was quantified from the

luminescence (relative light units; RLU) after subtracting the background from the no-enzyme control and comparing the value to a standard curve (Fig. S3). Graph titles indicate the growth medium and the substrate constituents of the reaction mixtures used to supplement the growth medium. The source of the protein extracts used in the reactions are in parentheses in bold typeface next to the strain genotype (*Rs*BluE reaction or vector resection). Representative graphs of two independent experiments performed in triplicate. Error bars represent the standard deviation from the mean. C and D. Growth analysis of *S. enterica* cells grown normoxically at 37°C in NCE minimal medium with glycerol (22 mM), $MgSO_4$ (1 mM), Cby (1 nM), and filter sterilized *Rs*BluE reaction mixtures (6% v/v) described above (reactions from panel B) containing either ATP (0.08 mM) and L-Thr (0.8 mM, panel C) or L-Ser (0.8 mM, panel D). The final concentrations of substrates after dilution of the filtered reaction mixtures into the medium are in parentheses. Graphs are representative of two independent experiments performed in triplicate. Error bars represent the standard error of the mean. Figure key: Panel C, D: (▲) *pduX*$^+$ strain supplemented with filter sterilized negative control enzymatic reaction containing ATP, and L-Thr (panel C) or L-Ser (panel D) and sarkosyl-solubilized protein extracts from cells carrying the empty vector; (◆) Δ*pduX* strain supplemented with filter sterilized negative control enzymatic reaction containing ATP, and L-Thr (panel C) or L-Ser (panel D) and sarkosyl-solubilized protein extracts from cells carrying the empty vector; (○) Δ*pduX* strain supplemented with filtered enzymatic reaction containing ATP, and L-Thr (panel C) or L-Ser (panel D) and purified sarkosyl-solubilized *Rs*BluE protein; (■) Δ*cobD* strain supplemented with filtered enzymatic reaction containing ATP and L-Thr (panel C) or L-Ser (panel D) and purified sarkosyl-solubilized *Rs*BluE protein.

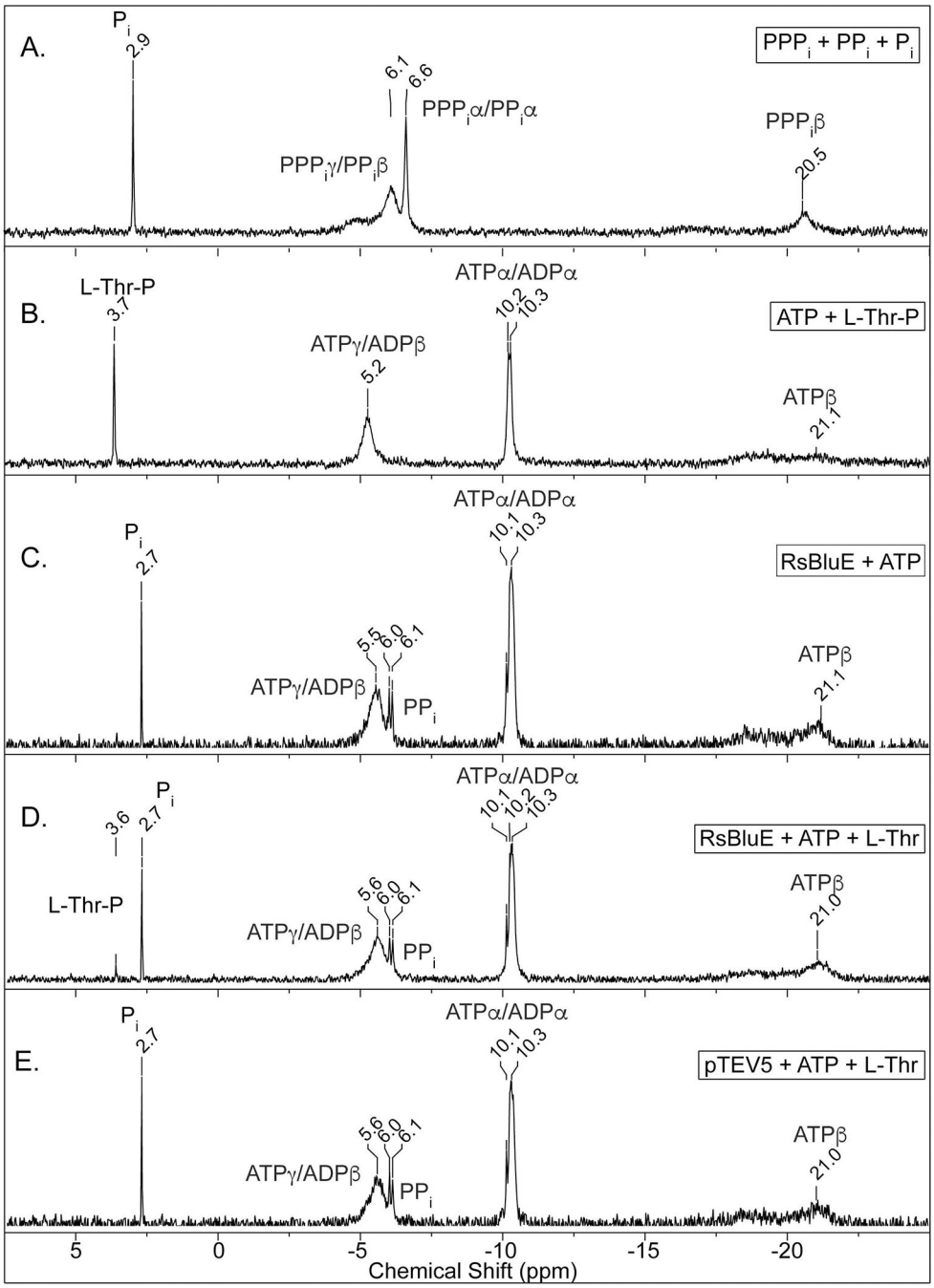

Figure 8. ^{31}P-NMR spectra of *Rs*BluE reaction products.

Representative ^{31}P-NMR spectra of duplicate independent experiments. Reaction mixtures containing $MgCl_2$ (1 mM), ATP (3 mM), L-Thr (6 mM), and 10 μL of detergent-free *Rs*BluE protein (11 μM) were incubated at 25°C for 1 h. A. No enzyme reactions with AMP, sodium *ortho*-phosphate (Pi), sodium pyrophosphate (PPi), and sodium polytriphosphate (PPPi) standards. B. No enzyme reactions with L-Thr-P and ATP standards. C. Reaction containing ATP and *Rs*BluE. D. Reaction containing ATP, L-Thr, and *Rs*BluE. E. Reaction

containing ATP, L-Thr, and extracts from cells carrying pTEV5 empty vector. Conditions used for the acquisition of the spectra are described in the *Materials and Methods* section.

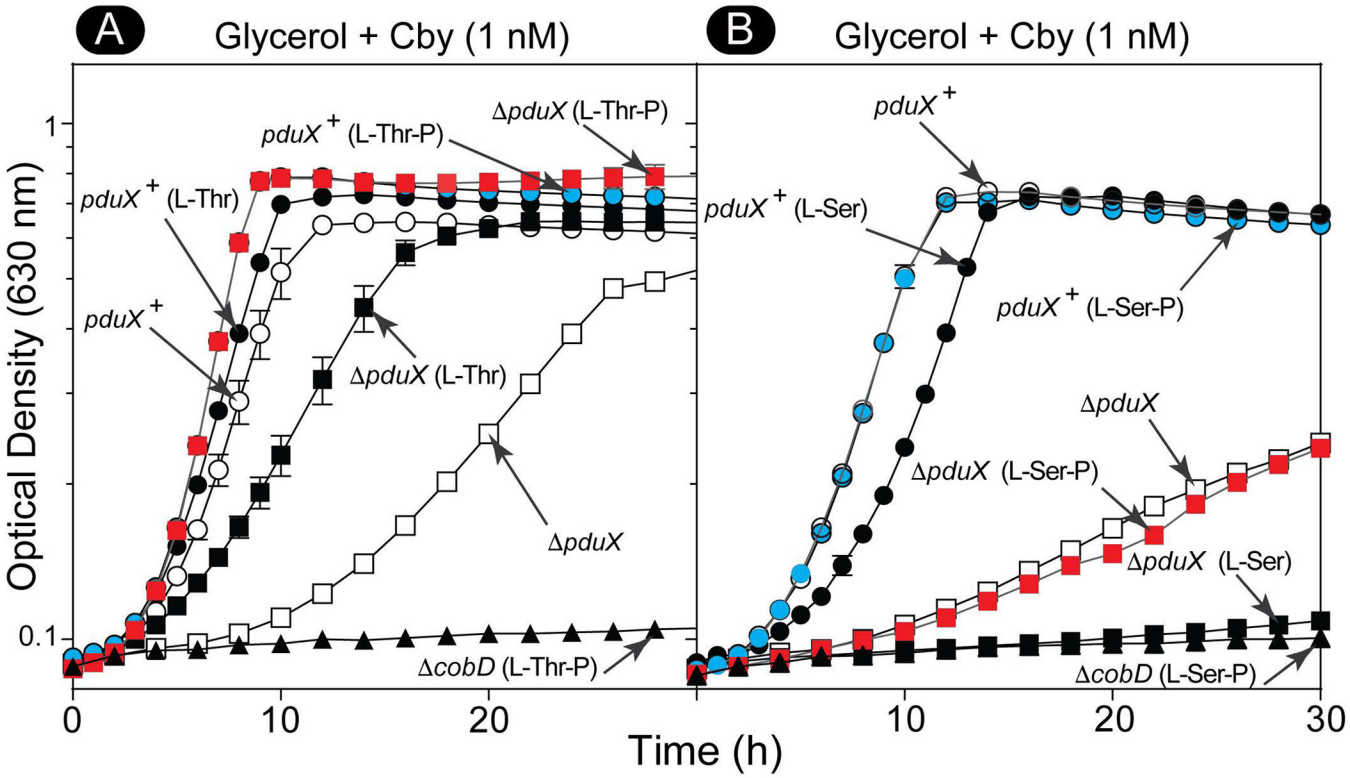

Figure 9. Growth analysis of *S. enterica* strains in the presence of L-Thr, L-Thr-P, L-Ser, and L-Ser-P.

Growth analysis of *S. enterica* cells grown normoxically at 37°C in NCE minimal medium with glycerol (22 mM), $MgSO_4$ (1 mM), and A. Cby (5 nM) supplemented with L-Thr or L-Thr-P (1 mM), or B. Cby (1 nM) supplemented with L-Ser or L-Ser-P (1 mM). The amino acid or phospho-amino acid supplement is indicated in parentheses next to the strain genotype. Representative graphs of two independent experiments performed in triplicate. Error bars represent the standard error of the mean. Figure key: Panel A: Δ*pduX* (□), Δ*pduX* (L-Thr) (■), Δ*pduX* (L-Thr-P) (■), *pduX*+ (○), *pduX*+ (L-Thr) (●), *pduX*+ (L-Thr-P) (●), Δ*cobD* (L-Thr-P) (▲), Panel B: Δ*pduX* (□), Δ*pduX* (L-Ser) (■), Δ*pduX* (L-Ser-P) (■), *pduX*+ (○), *pduX*+ (L-Ser) (●), *pduX*+ (L-Ser-P) (●), Δ*cobD* (L-Ser-P) (▲).

Table 1.

Comparison of *Rs*BluE and *Se*PduX activities as a function of substrates.

Specific activity values for purified and sarkosyl solubilized *Rs*BluE and *Se*PduX enzymes were assayed for ATPase activity in the presence and absence of L-Thr or L-Ser. Values are reported as mean ± standard deviation of three measurements of activity at 100 mM ATP and 50 mM L-Thr or L-Ser. Activity was measured with a NADH consumption assay (see *Materials and Methods*).

Protein	ATP (μmol ATP min^{-1} mg^{-1})	L-Thr (μmol ATP min^{-1} mg^{-1})	L-Ser (μmol ATP min^{-1} mg^{-1})
*Rs*BluE	0.93 ± 0.02	0.77 ± 0.02	0.42 ± 0.01
*Se*PduX	1.00 ± 0.03	0.91 ± 0.03	0.65 ± 0.02